UNIVERSITY OF CRAIOVA

FACULTATY OF MATHEMATICS AND NATURAL SCIENCES

DOCTORAL SCHOOL OF EXACT SCIENCES

DOMAIN: PHYSICS

CANCEA Virgil-Nicolae

OXIDIC THIN FILMS WITH FUNCTIONAL PROPERTIES OBTAINED BY LASER TECHNIQUES

Abstract of PhD thesis

PhD supervisor,
Sc. Res. Deg. I Dr. DINESCU Maria

CRAIOVA
2014

CONTENTS

1. INTRODUCTION

Metallic oxides are interesting materials, endowed with physical and chemical properties suitable to a wide palette of applications. ***Zirconium dioxide nanostructures (ZrO_2)*** and ***titanium dioxide nanostructures (TiO_2)*** exhibit various applications in electronics, nuclear waste management, microfluidics, environmental procedures, fabrication of everyday consumer goods, implants, prosthetics, but also in novel, interdisciplinary specialized subdomains, situated at the confluence between physics and other sciences, like bionanotechnologies or nanobiomedicine.

On the other hand, ***pulsed laser deposition*** **(PLD)** and ***matrix-assisted pulsed laser evaporation*** **(MAPLE)** – versions of physical vapor depositions – stand for some of the most promising techniques used at the formation of complex oxide heterostructures, super-lattices, and optimally controlled interfaces.

This thesis is focused on the ***laser-based synthesis of two classes of oxide thin films (zirconia and titania) with functional properties recommending them to applications in cutting-edge scientific and technological domains such as cell and molecular biology, nuclear waste management, bionanotechnologies and biomedicine***. It is structured into ***six chapters and author's cumulated bibliography***, among which the first is introductive and the sixth conclusive. Chapters 2, 3, 4, and 5 expose the author's original contributions and are based on *eleven papers written in collaboration*, among which *two published in ISI journals, three published in journals indexed in international databases,* and *six presented at specialized international conferences*.

Two laser systems were employed: one ArF – COMPexPro 205 F from Coherent (wavelength 193 nm, repetition rate 40 Hz, pulse duration 25 ns) and the other Nd:YAG Surelite SL II-10 produced by Continuum Company (at the fundamental wavelength, 1064 nm, and at the fourth harmonic, 266 nm, repetition rate 10 Hz, pulse duration 5 – 7 ns). Concerning the RF-PLD technique, the plasma source is generated within a two-chamber discharge system endowed with a radio-frequency power generator (13.56 MHz, CESAR 1310, maximum RF power 1000 W) and the plasma beam is admitted into the ablation chamber orthogonally to the target by an aperture cut into the lower electrode.

The ***XRD*** (X-Ray Diffraction) ***analysis*** of the deposited samples has been acquired by a PANalytical's X'Pert PRO MRD (Materials Research Diffractometer) system with standard θ–2θ Bragg-Brentano diffraction geometry using Cu K_α emission radiation (λ=0.15418 nm), with a step 2θ=0.02°, and an acquisition time interval of 4s per step. ***AFM*** (Atomic Force Microscopy) ***imaging*** has been done by a XE-100 Park Systems microscope with a maximum and respectively minimum scanning area of 50x50 μm^2 and respectively 500x500 nm^2 together with a maximum vertical scan range of 12 μm in non-contact mode (NC-AFM). The ***SIMS*** (Secondary Ion Mass Spectrometry) ***equipment*** (Hiden Analytical) is endowed with an Argon ion gun (maximum energy 5 keV, maximum current intensity 100 mA, source gas pressure 3×10^{-5} mbar), the secondary ions being filtered by a quadrupole mass analyzer. Two types of analyses have been performed: *mass spectra* by irradiating a small area, of 20×20 μm^2, of each sample with a primary ion beam of low intensity (1-2 nA) and *depth profiles* by irradiating a larger area, of 300×400 μm^2, of each sample with a primary ion beam of higher intensity (460 nA). ***SE*** (spectroscopic ellipsometry) ***characterization*** has been carried on by

means of polarimetric techniques using a J. A. Woollam V-VASE (Vertical-Variable Angle Spectroscopic Ellipsometer) system equipped with a HS-190 scanning monochromator and a high pressure Xe discharge lamp, which generates light within the spectral range from near IR to UV, 250 – 1700 nm, with a step of 2 nm.

Chapter 2 exposes the synthesis and characterization of functional ZrO_2 thin films applicable to cell and molecular biology. These films have been deposited by PLD on Si (100) substrates by means of an ArF laser under various conditions and have been characterized physically from the point of view of their crystal structure (XRD), surface morphology (AFM), composition (SIMS), and optical behavior (SE). Their biological properties have also been investigated by performing *in-vitro* biocompatibility adherence tests of a specific adult mouse fibroblast cell line (L929) grown on the zirconia thin film surfaces, accompanied by further chemical and biochemical analyses. The optimal (from the perspective of biological applications) PLD synthesis of ZrO_2 thin films has been accomplished in the following experimental configuration: at a laser fluence of 3.4 J/cm^2, applying 80,000 laser pulses, at a substrate temperature of 600 °C, in O_2 background gas at 0.01 mbar, and in the presence of a RF plasma discharge power of 100 W. The main characteristics of the thin films prepared according to these specifications can be synthesized as follows: 1. Regular nanostructured surfaces, displaying a distribution of grain sizes within the range 40 – 70 nm; 2. Polycrystalline monoclinic surfaces, thermodynamically stable; 3. Porous thin films with an inhomogeneous stratification; 4. Very good optical properties; 5. Chemical stability in the presence of typical antibiogram reactives; 6. Bacteriostatic effect in the presence of an Escherichia coli culture; 7. *in-vitro* biocompatibility properties manifested by a high adherence of L929 cells to the film surfaces.

Chapter 3 analyzes the formation of functional ZrO_2 thin films with applications to nuclear waste management. Micrometric/nanometric crystalline thin films have been obtained by PLD on Si(100) collectors using a Nd:YAG laser under various conditions and at a fixed value of the laser fluence – 2.5 J/cm^2. Some of the films have been grown by RF-PLD at 100 W. The resulting thin films have been characterized via XRD, AFM, NRBS (non-Rutherford Backscattering Spectrometry), and SE techniques. The main conclusions on their properties can be synthesized into: 1. Tetragonal zirconia crystalline phase is prevalently formed at a substrate temperature of at least 400 °C, in which context the peaks associated with the reflections t(101) and t(002) are the most visible; 2. Surface morphology modifies insignificantly under substrate temperature variations: spare droplets are observed and the RMS roughness values are stabilized to approximately 6 nm for all the films; 3. Average composition and thickness values of the zirconia layers following from alpha backscattering spectra are given by $ZrO_2Hf_{0.012}$ and respectively by 1300 x 10^{15} atoms/cm^2; 4. RF-assistance of the PLD process improves the surface quality by lowering the roughness values and droplet sizes simultaneously with a more pronounced film surface nanostructuring than in the case of conventional PLD. 5. Optimal optical properties are exhibited with respect to the films deposited at 600 °C by RF-PLD (P_{RF}=100 W).

Chapter 4 is dedicated to the growth of functional TiO_2 thin films with applications to bionanotechnologies. The films have been synthesized by both PLD and MAPLE techniques using Si(100) and respectively PPX-coated Si(100) substrates. The growths by PLD have been done with two laser systems: one ArF and the other Nd:YAG. In view of the MAPLE

technique the targets were previously prepared by freezing some aqueous TiO_2 powder solutions of different weight concentrations. In this case a Nd:YAG laser system was employed. The deposited TiO_2 films have been investigated by XRD, AFM, SIMS, and SE. The effect of the substrate topography on the wettability properties of the TiO_2 thin layers has been analyzed by contact angle measurements (CAM). The main conclusions are as follows: 1. Morphology of titania films grown by PLD is characterized by smooth, uniform surfaces, whose roughness increases with an increase in the laser operating wavelength. On the other hand, MAPLE favors an increase of the film roughness with the TiO_2 target concentration irrespective of the substrate morphology; 2. PLD synthesis ensures a more balanced film composition by contrast to the inhomogeneous depositions produced by MAPLE; 3. Crystallinity lacks or is rather poor. Anatase phase is identified, but only for MAPLE growths from high concentration TiO_2 targets; 4. PLD-emerging samples exhibit very small values of their extinction coefficients together with values of the refraction index close to those reported in the literature, while MAPLE-grown films are less transparent and with lower values of the refraction index on a broad spectral range; 5. Substrate properties decisively influence the TiO_2 film wettability: parylene-coated Si(100) collectors lead to more hydrophilic surfaces than plain Si(100) supports.

Chapter 5 focuses on the preparation of functional TiO_2 thin films with applications to implantology and prosthetics. Such thin layers have been synthesized by PLD with an ArF laser on three types of substrates: BK7 optical glass, Si(100), and quartz. Their physical characterization has been instrumented by XRD, AFM, SIMS, and SE. The accompanying bio-medical properties have been investigated via four *in-vitro* biocompatibility tests of a cell line L929 grown on the surfaces of the samples collected on optical glass: adherence, viability, and detection of the TiO_2 film genotoxic potential by means of alkaline comet and respectively cytokinesis-block micronucleus assays. The ablation configuration of the TiO_2/glass films that proved optimal with respect to the envisaged biomedical applications is characterized by: laser fluence – 3.4 J/cm^2, number of laser pulses applied on the target – 80,000, substrate temperature – 300 °C, in an O_2 background at 0.01 mbar, and with RF assistance (100 W). The main properties of the thin films prepared in this manner are synthesized by: 1. Formation of nanostructured surfaces with well-delimited pores presenting an average diameter of approximately 200 nm, a relatively high RMS roughness, of approximately 5 nm on a 20x20 μm^2 AFM scanning area, but without a noticeable crystalline organization; 2. Production of porous films with an inhomogeneous stratification, but with a better stoichiometry than in the case of samples deposited either in vacuum or without RF assistance; 3. Good optical properties, materialized in films transparent with respect to the visible and near IR radiation and possessing relatively high values of both the refraction index and transmittance; 4. Remarkable *in-vitro* biocompatibility features in the presence of L929 cell cultures, defined by A. an increased attachment level of these cell to the titania surfaces; B. an intense bioactivity (elevated viability); C. an inobservable genotoxic potential, as follows from the results of both alkaline comet and cytokinesis-block micronucleus assays.

The results exposed so far allow for ***further perspectives*** at the level of pulsed laser synthesis, characterization, and biocompatibility properties of TiO_2-ZrO_2 thin films mixed in various proportions.

2. FUNCTIONAL ZIRCONIUM DIOXIDE THIN FILMS WITH APPLICATIONS TO BIOLOGY

Zirconium dioxide has been intensively studied lately from the perspective of its biocompatibility properties, especially of its enormous potential of applications in dentistry, as inlays, onlays, full crowns, bridges, abutments, intra-root posts, in tissue engineering at the construction of scaffolds, and in implantology [1,2].

In this context, chapter 2 exposes the synthesis and characterization of functional ZrO_2 thin films applicable to cell and molecular biology. These films have been deposited by PLD on Si(100) substrates by means of an ArF laser under various conditions using a ceramic ZrO_2 (doped with Hf 2.5%) target and have been characterized physically from the point of view of their crystalline structure (XRD), surface morphology (AFM), composition (SIMS), and optical behavior (SE). Some of the films have been grown by RF-assisted pulsed laser deposition (RF-PLD), in which case the RF power was fixed at 100 W [3]. Their biological properties have also been investigated by performing *in-vitro* biocompatibility adherence tests of a specific adult mouse fibroblast cell line (L929) grown on the zirconia thin film surfaces [4,5], accompanied by further chemical and biochemical analyses.

2.1. FILM SYNTHESIS

The deposition experiments by either PLD or RF-PLD of ZrO_2 thin films are synthesized in **Table 1**.

Table 1. *Experimental conditions used at the synthesis of ZrO_2 thin films.*

Sample No.	Target	Substrate	Oxygen pressure (mbar)	d_{t-s} (cm)	$T_{subst.}$ (°C)	E_{laser} (mJ)	N_{pulses}	Spot area (mm^2)	Φ (J/cm^2)	P_{RF} (W)	λ (nm)
1157a	ZrO_2	Si(100)/ photoresist	10^{-6}	4	RT	17	40,000	0.5	3.4	0	193
1157b	ZrO_2	Si(100)	10^{-6}	4	RT	17	40,000	0.5	3.4	0	193
1158	ZrO_2	Si(100)	10^{-6}	4	300	17	80,000	0.5	3.4	0	193
1159	ZrO_2	Si(100)	10^{-6}	4	600	17	80,000	0.5	3.4	0	193
1160	ZrO_2	Si(100)	0.01	4	RT	17	80,000	0.5	3.4	0	193
1161	ZrO_2	Si(100)	0.01	4	300	17	80,000	0.5	3.4	0	193
1162	ZrO_2	Si(100)	0.01	4	600	17	80,000	0.5	3.4	0	193
1163	ZrO_2	Si(100)	0.01	4	RT	17	80,000	0.5	3.4	100	193
1164	ZrO_2	Si(100)	0.01	4	300	10	80,000	0.5	2.0	100	193
1165	ZrO_2	Si(100)	0.01	4	300	17	80,000	0.5	3.4	100	193
1166	ZrO_2	Si(100)	0.01	4	600	17	80,000	0.5	3.4	100	193

2.2. RESULTS AND DISCUSSIONS

The dependence of ***film crystallinity*** on the substrate temperature is clear from **Figure 1a** in the sense that the higher the temperature the more accurate the crystal phase. While for films deposited at RT only an amorphous peak around 2θ=30° is present, for films grown at 300 °C there appear some broad diffraction maxima, but not so clearly defined, accredited to the tetragonal crystal phase of zirconia (file JCPDS 01-75-7115) and respectively to the reflection (-111) of the monoclinic ZrO_2 phase (file JCPDS 01-70-2491). On the contrary, for films synthesized at 600 °C both crystal phases are clear, exhibiting a long-range crystal organization. The tetragonal phase is dominant for films deposited at 600 °C, while for those grown at 300 °C the fraction of monoclinic phase is prevailing. For the samples prepared under RF sputtering at a temperature of 600 °C (crystallization-favorable) it is observed the formation of the same two ZrO_2 crystal phases – tetragonal and monoclinic (**Figure 1b**), but with an obvious increase in the proportion of the monoclinic phase, which is thermodynamically more stable. Several maxima pertaining to the monoclinic phase have been recorded within the diffraction spectra of thin films deposited in the presence of RF, suggesting therefore the formation of a polycrystalline monoclinic phase. **Figure 1c** displays the comparative analysis of X-Ray spectra for ZrO_2 samples deposited at the same substrate temperature of 600 °C, but either in presence of oxygen background at 0.01 mbar or in vacuum. In the case of vacuum conditions one observes the formation in a leading proportion of a tetragonal phase in which the (002) reflection is also visible. The monoclinic maximum (-111) is less intense, so one can conclude that vacuum conditions are best for obtaining the largest fraction of tetragonal phase.

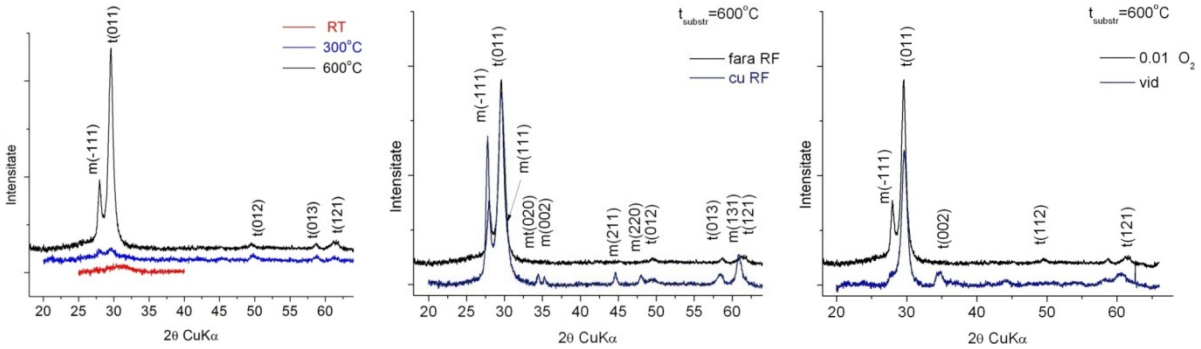

Figure 1. *X-ray diffractograms of ZrO_2/Si(100) samples: (a) (left) at various substrate temperatures: 1160 (red), 1161 (blue), and 1162 (black); (b) (middle) with/without RF: 1162 (black) and 1166 (blue); (c) (right) vacuum/O_2 background gas: 1159 (blue) and 1162 (black).*

Related to the ***AFM characterization*** of zirconia samples, the deposition rate has initially been evaluated within the range 0019 – 0.002 nm/pulse. Subsequently, the influence of the deposition parameters on the surface morphology of ZrO_2 films has been investigated. The influence of the RF discharge (in O_2 background and at 600 ºC) is shown in **Figure 2**. In the absence of RF assistance larger grains (with dimensions within 40 – 90 nm) are formed and the roughness is valued at 0.6 nm (**Figure 2a**). On the contrary, the presence of RF discharge leads to an observable nanostructure of ZrO_2 thin films, with a roughness of 0.9 nm, while on small scanning areas there appear regular grains with a diameter (in the horizontal plane) between 40 and 70 nm (**Figure 2b)**. Thus, it seems that the presence of RF

treatment induces a larger roughness simultaneously with the formation of a more regular nanostructure.

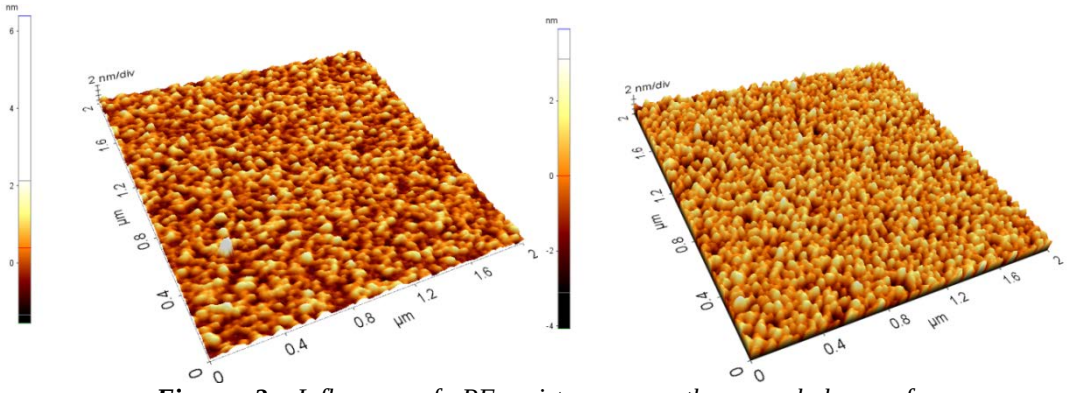

Figure 2. *Influence of RF-assistance on the morphology of ZrO_2/Si(100) thin films: (a) (left) sample 1162, without RF – RMS: 0.6 nm; (b) (right) sample 1166, with RF – RMS: 0.9 nm.*

The substrate temperature is another key factor that affects the topography of zirconia thin films, as can be seen from **Figure 3**. Two samples are analyzed – both grown in O_2 background gas and with RF assistance: 1163 deposited at RT and 1166 prepared at 600 ºC. The comparison between the two sets of AFM images indicates that an increase of the substrate temperature from RT to 600 ºC leads to a decrease of the RMS roughness from 8 nm to 0.9 nm on 5x5 µm^2 and respectively from 6 nm to 0.6 nm on 20x20 µm^2, in parallel with smaller values of grain dimensions. Meanwhile, the surface aspect tends to be more nanostructured with an increase of the temperature. In other words, the heating of the substrate in O_2 atmosphere combined with RF assistance represent some treatments that favor the lowering of both grain dimensions and ZrO_2 thin film roughness.

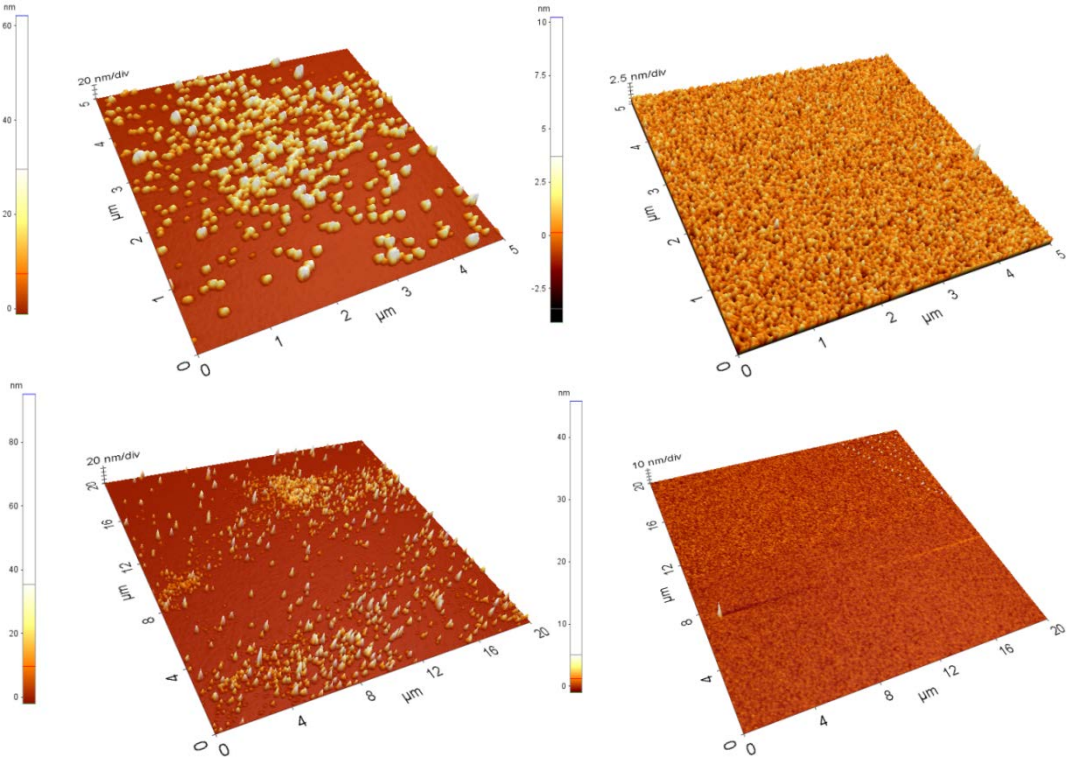

Figure 3. *Influence of substrate temperature on the morphology of ZrO_2/Si(100) thin films grown by RF-PLD: on 5x5 µm^2 – (a) (left-up)*

sample 1163, deposited at RT – RMS: 8 nm; (b) (right-up) sample 1166, deposited at 600 °C – RMS: 0.9 nm; on 20x20 μm^2 – (c) (left-down) sample 1163, deposited at RT – RMS: 6 nm; (d) (right-down) sample 1166, deposited at 600 °C – RMS: 0.6 nm.

In order to realize the ***compositional characterization*** of zirconia thin films prepared by PLD the depth profiles of three samples synthesized under different conditions (1159 – vacuum, 600 °C; 1166 – O_2 background, 600 °C, with RF; 1160 – O_2 background, RT, without RF) have been compared. It can be seen that the thicknesses of the first two films are greater than that of the last. On the other hand, samples 1159 and 1160 exhibit a relatively uniform distribution of their constituents (^{16}O, ^{28}Si, ^{90}Zr), unlike sample 1166, which proves an obvious imbalance among the same depth components (**Figure 4**). The time evolution of the oxygen and respectively zirconium signals is different, which can be explained by the fact that samples 1159 and 1160 are more homogeneous, while 1166 seems to be composed of two layers of different densities: an inner one, onto the Si(100) substrate, and an outer one, rougher than the former and placed on top of it.

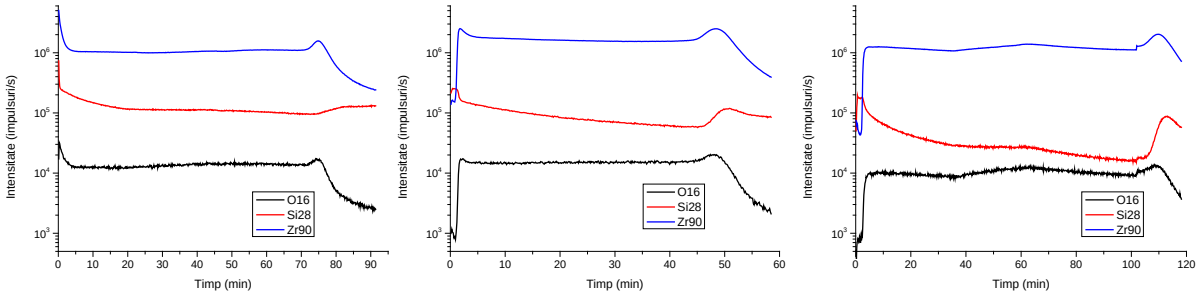

Figure 4. *Depth profiles of ZrO_2/Si(100) thin films illustrating different homogeneity degrees: (a) (left) 1159 – 600 °C, vacuum; (b) (middle) 1160 – RT, O_2 background, without RF; (c) (right) 1166 – 600 °C, O_2 background, with RF.*

The ***optical/dielectric characterization*** has been performed at fixed incidence angles, of 60°, 65°, and 70°. The calculation of geometric (film thickness, roughness) and optical parameters (refraction index *n* and extinction coefficient *k*) of the zirconia thin films debuted with a 4-layer optical model composed of the Si(100) collector (with a thickness of about 1 mm), a native SiO_2 layer (approximately 3-nm-thick), the ZrO_2 thin film, and the roughness layer taken as BEMA 50% ZrO_2 – 50% air and was based on a two-step fitting procedure. The thickness of each ZrO_2 film and of the corresponding roughness layer together with the intermediate values of *n* on the spectral subinterval 500 – 1700 nm where ZrO_2 is transparent [6] were initially obtained assuming a two-parameter Cauchy dispersion law [7,8]. Then, the function *n* was constructed on the entire investigated wavelength spectrum, 250 – 1700 nm, under the hypothesis of anomal Gauss dispersion and assuming the geometric parameters from the first step. **Table 2** includes the emerging values of the Gauss fitting parameters.

Table 2. *Gauss fitting parameters for the ZrO_2/Si(100) thin films.*

Sample	Amp	En (eV)	Br (eV)	MSE
1159	7.0779±0.0894	13.966±0.295	8.9853±0.263	72.41
1162	13.443±0.112	9.4408±0.027	3.7031±0.0386	5.099
1163	19.849±5.15	8.9932±0.137	1.9394±0.525	4.533
1164	11.985±0.048	9.6448±0.0188	4.1471±0.0225	3.786

1165	20.196±1.41	8.841±0.0585	2.2913±0.171	9.675
1166	16.331±0.338	9.1236±0.0346	2.9503±0.0698	9.783

Figure 5 includes the graphic representations of *n* and *k* on the entire spectral range according to the Gauss fitting for samples deposited under the same conditions excepting the substrate temperature. Higher values of the refraction index are observed at 300 °C and respectively at 600 °C than at RT. The values of the extinction coefficients are small, and therefore these thin films are practically transparent over the entire spectral range.

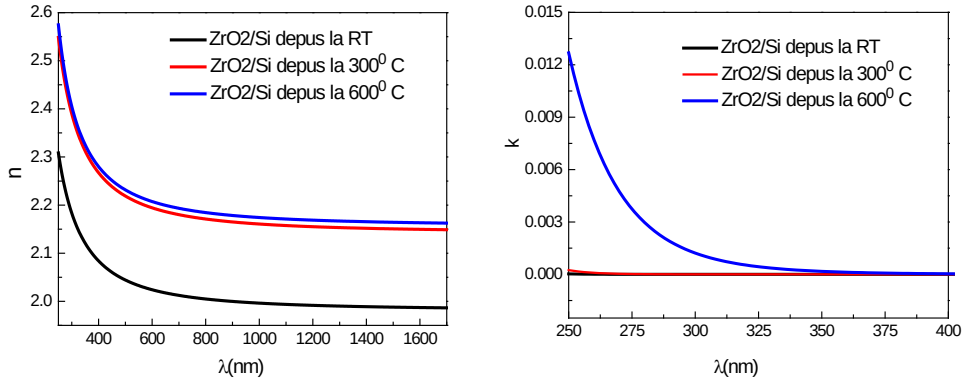

Figure 5. *Dependence of n (left) and k (right) on the wavelength for ZrO_2/Si(100) samples deposited in O_2 background, with RF, under different substrate temperatures – 1163 (black), 1165 (red) and 1166 (blue).*

For samples grown at 600 °C (**Figure 6**) in various conditions smaller values of *n* are noticed for vacuum depositions compared to those in O_2 background, while the RF assistance (maintaining the O_2 background gas) does not affect the values of the refraction index. By contrast, *k* is influenced: the RF treatment favors a more reduced absorption of photon energy.

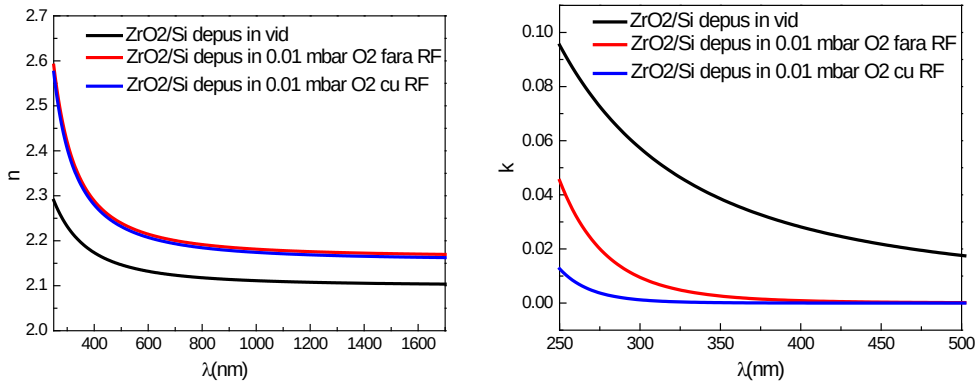

Figure 6. *Dependence of n (left) and k (right) on the wavelength for ZrO_2/Si(100) samples deposited in various conditions, but at 600 °C – 1159 (black), 1162 (red) and 1166 (blue).*

In view of performing the *in-vitro* biocompatibility tests by ***evaluating the cell morphology – computation of cell adhesion with respect to these thin films*** – three ZrO_2/Si(100) samples have been selected: 1159 (vacuum, 600 °C), 1160 (O_2 – 0.01 mbar, RT), and 1166 (O_2 – 0.01 mbar, 600 °C, RF – 100 W). An adult mouse fibroblast cell line L929 (Sigma-Aldrich) at passage 20 was employed. A cell culture was initially prepared according to the standard protocols [4,5] resulting in a suspension of 100,000 L929 cells per mL in growth medium (L-glutamine, 10% FCS). The samples were autoclaved (120 °C, 30 min.) and placed together with a plastic control in triplicate on a labeled TPP 12-well tissue

culture test plate. On each surface was added an initial volume of 100 µL of the prepared cell suspension (10,000 cells per sample). Labeled slides assembled on the tissue culture test plate were kept to adhere for 30 minutes by incubation (37 °C, CO_2 5%, humidity). Cells were then incubated (37 ºC, 5% CO_2, and humidity) for 20 hours in a growth medium volume of 1.5 ml for each well (MEM, 10% FCS, L-glutamine). The 12-well culture test plate was then removed from the incubator, cells were washed with PBS (Phosphate buffered saline), immediately fixed by incubation in 3% paraformaldehyde, washed again with PBS, incubated for 15 min. with Acridine Orange, washed once more with PBS, and finally dehydrated by ethanol baths of increasing concentrations (50%, 80%, 96%). Subsequently the sample and control surfaces were investigated with an optical microscope Olympus BX51 equipped with an adequate filter (**Figure 7**).

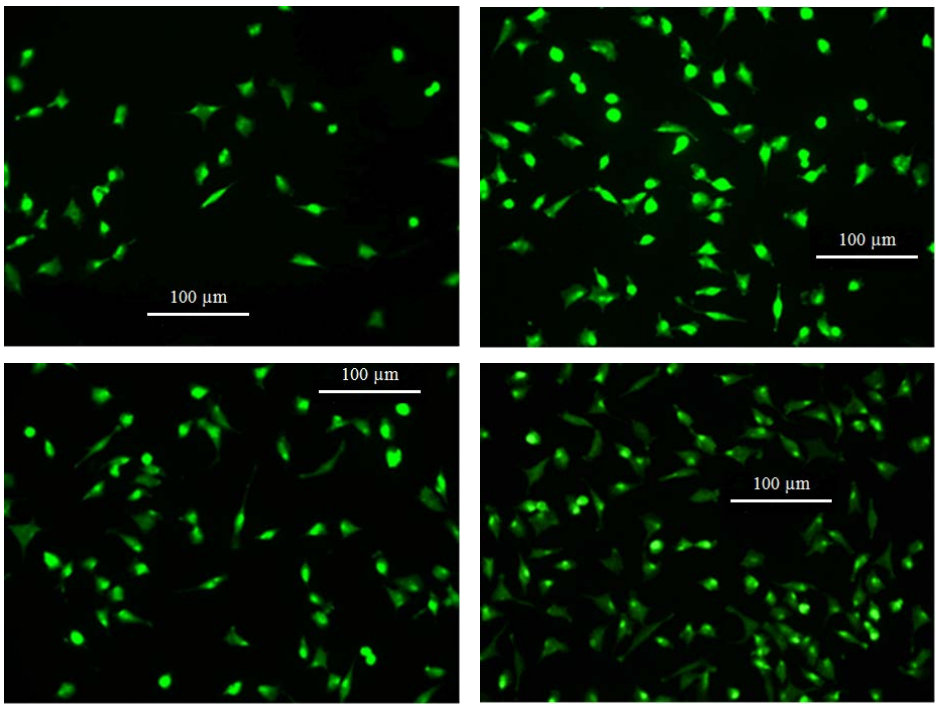

Figure 7. *In-vitro adherence of L929 cells to the investigated surfaces: (a) (left-up) plastic control, (b) (right-up) sample 1159, (c) (left-down) sample 1160, (c) (right-down) sample 1166.*

The quantitative estimation of adherence requires cell counting according to their morphological classification into *round* and *spread* cells [5,9,10]. The spread cells are well attached (they extend and acquire a dendritic form), so their presence defines the adherence property [9]. The *cell-spread ratio* [9], defined as the percentage of the number of spread cells to the specific total number of cells, is computed. The specific total number of cells considers only the round cells undergoing apoptosis processes and also the spread cells, but not the round cells involved in cell divisions (close one to another). The calculation of this quantity with respect to the above images leads to the values presented in **Figure 8**. It can be seen that the substrate temperature does not affect the adherence of L929 cells to the thin film surfaces, but the presence of oxygen background under pressure favors the attachment of these cells to the ZrO_2 surfaces. The maximum spread-cell ratio is attained for sample 1166, mainly due to the supplementary RF discharge treatment applied to this film during the synthesis process, which takes place also in the presence of an O_2 flux and therefore enhances the concentration

of oxidant gas compared to sample 1160. In consequence, the RF-PLD technique ensures the best adhesion properties of L9292 cells to ZrO_2 thin film surfaces.

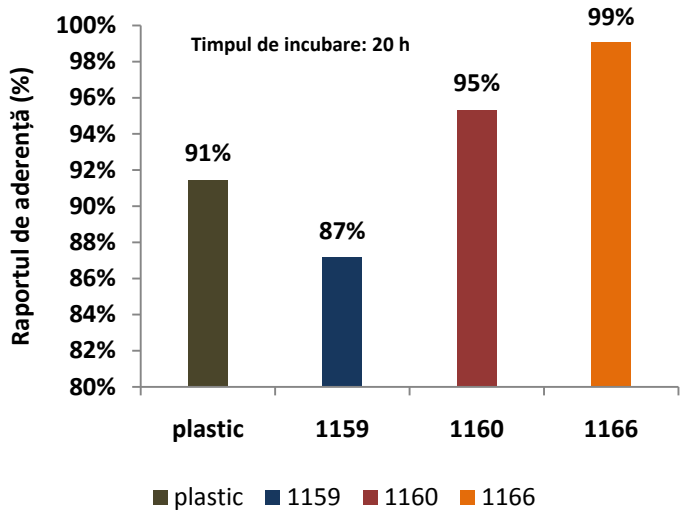

Figure 8. *Values of the cell-spread ratio of L929 cells as an indicator of cell adhesion to the control and respectively to the investigated ZrO_2/Si(100) samples.*

2.3. CONCLUSIONS

The optimal PLD synthesis of ZrO_2 thin films from the perspective of biological applications has been accomplished at a laser fluence of 3.4 J/cm^2, by applying 80,000 laser pulses, at a substrate temperature of 600 °C, in O_2 background gas at 0.01 mbar, and in the presence of a RF plasma discharge power of 100 W. The main properties of the thin films prepared accordingly can be synthesized into: 1. Regular nanostructured surfaces, displaying a grain size distribution within the range 40 – 70 nm; 2. Polycrystalline monoclinic surfaces, thermodynamically stable; 3. Porous thin films with an inhomogeneous stratification; 4. Very good optical properties; 5. Chemical stability in the presence of typical antibiogram reactives; 6. Bacteriostatic effect in the presence of an Escherichia coli culture; 7. *in-vitro* biocompatibility properties manifested by a high adherence of L929 cells to the film surfaces.

2.4. SELECTED BIBLIOGRAPHY

[1] J. OLIVA, X. OLIVA, J. D. OLIVA, *Int. J. Oral Maxillofac. Implants* **22** (2007) 430–435.
[2] P. F. MANICONE, P. ROSSI IOMMETTI, L. RAFFAELLI, *J. Dent.* **35** (2007) 819–826.
[3] G. DINESCU, B. MITU, E. ALDEA, M. DINESCU, *Vacuum* **56** (2000) 83–86.
[4] R. I. FRESHNEY, *Culture of Animal Cells: A Manual of Basic Technique and Specialized Applications*, 6th edition, Boston: Wiley-Blackwell, 2010.
[5] C. D. HELGASON, C. MILLER, *Basic Cell Culture Protocols*, 4th edition, Springer Protocols, Methods in Molecular Biology Series, vol. **946**, New York: Humana Press, 2013.
[6] W. ZHAMG, J. GAN, Z. HU *et al.*, *Appl. Spectrosc.* **65** (2011) 522–527.
[7] H. G. TOMPKINS, E. A. IRENE (Editori), *Handbook of Ellipsometry*, William Andrew, Inc., Springer Verlag, 2005.
[8] H. FUJIWARA, *Spectroscopic Ellipsometry: Principles and Applications*, John Wiley & Sons Ltd., 2007.
[9] T. TANAKA, Y. SUZUKI, K. TSUCHIYA, H. YAJIMA, *Appl. Surf. Sci.* **265** (2013) 281–285.

[10] B. ALBERTS, A. JOHNSON, J. LEWIS, M. RAFF, K. ROBERTS, P. WALTER, *Molecular Biology of the Cell*, 4th edition, New York: Garland Science, 2002.

3. FUNCTIONAL ZIRCONIUM DIOXIDE THIN FILMS WITH APPLICATIONS TO NUCLEAR WASTE MANAGEMENT

Nuclear waste management is one of the foreground fields responsible with life and environment protection, its main preoccupation being focused on the elimination of excess plutonium stemming from nuclear power plants and nuclear weapon dismantling. One of the viable options is represented by the incineration in a light water reactor [1] and use of inert fuel matrices. Zirconia in particular exhibit attracting features in this context due to its elevated melting point [2], stability to irradiation [3], high chemical stability [4], low solubility in water, enhanced retention of radiotoxic elements, and adequate neutron properties [5].

Chapter 3 analyzes the formation of functional ZrO_2 thin films with applications to nuclear waste management. Micrometric/nanometric crystalline thin films have been obtained by PLD on Si(100) collectors using a Nd:YAG laser under various conditions at a fixed value of the laser fluence – 2.5 J/cm^2. Some of the films have been grown by RF-PLD at 100 W. The resulting thin films have been characterized via XRD, AFM, NRBS (non-Rutherford Backscattering Spectrometry), and SE techniques.

3.1. FILM SYNTHESIS

The synthesis of zirconia thin films was acquired by pulsed laser ablation of a ZrO_2 ceramic target (stabilized with Hf) using a Nd:YAG system in various conditions (**Table 1**).

Table 1. *Experimental conditions used at the synthesis of ZrO_2 thin films.*

Sample No.	Target	Substrate	Oxygen pressure (mbar)	d_{t-s} (cm)	T_{subst} (°C)	N_{pulses}	Φ (J/cm^2)	P_{RF} (W)	λ (nm)
PLD569	ZrO_2	Si(100)	0.05	5	200	20,000	2.5	0	266
PLD570	ZrO_2	Si(100)	0.05	5	400	20,000	2.5	0	266
PLD571	ZrO_2	Si(100)	0.05	5	400	20,000	2.5	100	266
PLD572	ZrO_2	Si(100)	0.05	5	200	20,000	2.5	100	266
PLD573	ZrO_2	Si(100)	0.05	5	600	20,000	2.5	0	266
PLD575	ZrO_2	Si(100)	0.05	5	24	20,000	2.5	0	266
PLD576	ZrO_2	Si(100)	0.05	5	24	20,000	2.5	100	266
PLD584	ZrO_2	Si(100)	0.05	5	600	20,000	2.5	0	266
PLD585	ZrO_2	Si(100)	0.05	5	600	40,000	2.5	0	266
PLD586	ZrO_2	Si(100)	0.05	5	600	60,000	2.5	0	266

3.2. RESULTS AND DISCUSSIONS

The ***XRD characterization*** of these zirconia samples required the identification of diffraction maxima according to the files PDF JCPDS-ICCD card no. 42-1164 for the ZrO_2 tetragonal phase and respectively card no. 37-1484 for the monoclinic one. The pre-ablation XRD pattern of the ZrO_2 ceramic target exhibits a predominant tetragonal phase (nine visible peaks) and traces of monoclinic phase. The post-ablation XRD spectrum reveals increased intensities of the tetragonal phase due to ZrO_2 re-crystallization processes and the almost disappearance of the monoclinic phase. Comparing the X-ray diffractograms of samples deposited under the same conditions excepting the substrate temperature (**Figure 1a**), it is clear the influence of temperature on the crystalline structure, manifested by the transition from an amorphous behavior at small temperatures (200 °C) to the presence of a main tetragonal phase beginning with 400 °C, the sharpest peaks being observed at 600 °C. Only the peaks associated with the reflections t(101) and t(002) are detected, and therefore a preferred growth orientation. Comparing the XRD patterns of three samples prepared in the same conditions excepting the number of pulses (**Figure 1b**), we notice that the high temperature (600 °C) induces a tetragonal crystalline character. The linear variation of film thickness with the number of pulses can be evidenced by: (a) the quasi-linear dependence of each of the intensities corresponding to the two maxima with the number of pulses, and (b) the proportionality between the variation of diffraction peak intensity and the film thickness.

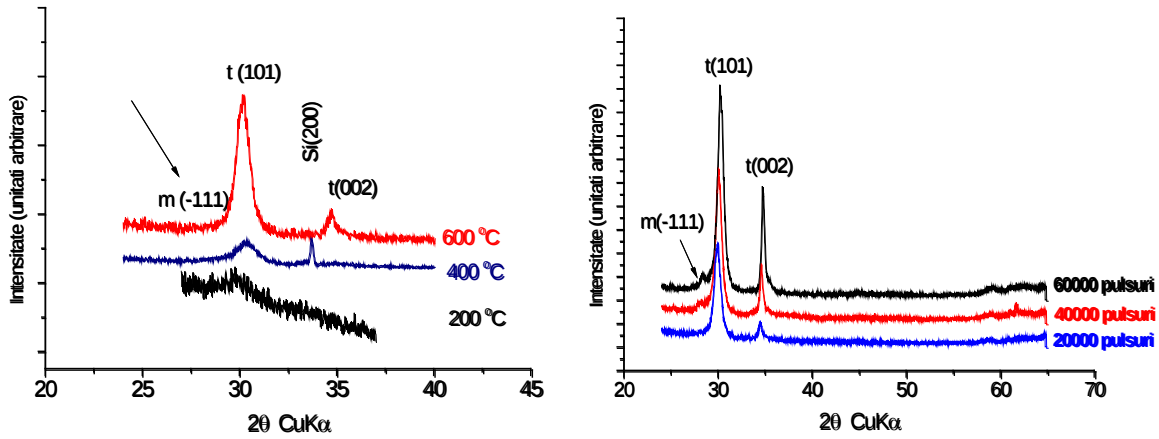

Figure 1. *XRD patterns of ZrO_2/Si(100) samples deposited at: (a) (left) different substrate temperatures: PLD569 (black), PLD570 (blue), and PLD573 (red); (b) (right) different values of the number of pulses: PLD584 (blue), PLD585 (red), and PLD586 (black).*

There is some anisotropy between the growths along two crystallographic directions of tetragonal zirconia corresponding to the reflections t(101) and t(002), highlighted by the different sizes of associated ZrO_2 crystallites computed with Scherrer's formula [6] (**Table 2**).

Table 2. *Evaluation of ZrO_2 crystallite sizes corresponding to two crystallographic growth orientations of the tetragonal phase.*

Sample no.	Substrate temperature (°C)	No. of laser pulses	D t(101) (nm)	D t(002) (nm)
Ceramic ZrO_2 target			34	34
PLD570	400	20,000	7	10

PLD573	600	20,000	10	21
PLD584	600	20,000	11	23
PLD585	600	40,000	11	24
PLD586	600	60,000	11	18

Next, we analyze the influence of substrate temperature and RF-assistance on the ***topography of zirconia samples***. Within the temperature range from 24 °C to 600 °C the surface morphology presented no significant changes (**Figure 2**) and therefore the substrate temperature does not affect the morphological properties of the deposited zirconia films.

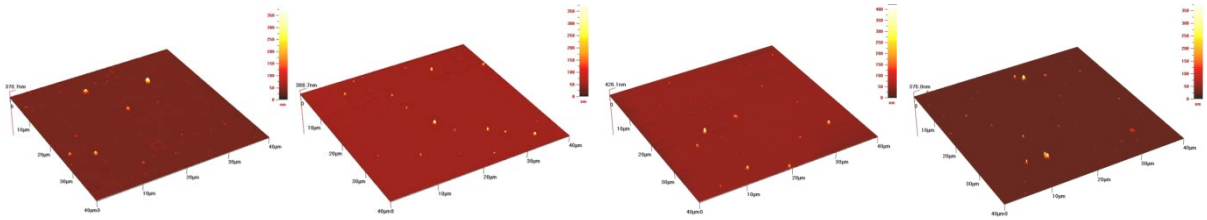

Figure 2. *Influence of substrate temperature on the morphology of ZrO_2/Si(100) samples: (a) (left) PLD575 – 24 °C; (b) (left-middle) PLD569 – 200 °C; (c) (right-middle) PLD570 – 400 °C; (d) (right) PLD573 – 600 °C.*

Regarding the impact of RF assistance on the morphology of ZrO_2 surfaces (**Figure 3**), one observes smaller values of both roughness and grain size than in the case of conventional PLD, while the grain distribution exhibits a lower density. Thus, it seems that the RF-PLD process ameliorates the quality of ZrO_2 thin film surfaces, in contrast to the variation of substrate temperature in the absence of RF power, which does not influence the surface properties.

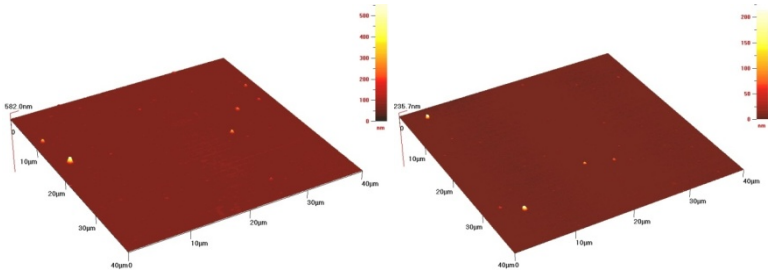

Figure 3. *Influence of RF assistance on the morphology of ZrO_2/Si(100) samples: (a) (left) PLD569 – without RF; (b) (right) PLD572 – with RF.*

In view of the ***compositional characterization*** of deposited thin films we used the non-Rutherford elastic backscattering spectrometry (NRBS) among the techniques based on ion beams (Ion Beam Analysis – IBA) [7]. In this framework the sample stoichiometry and thickness were determined. The NRBS measurements were carried out at a tandem Van de Graaff accelerator (8.5 MV) with a $^4He^{++}$ beam (4.5 MeV) and in the presence of a Si-based detection system placed at 167°. The incident beam energy exceeds the threshold up to which the Rutherford formula for oxygen (2.5 MeV) and silicon (3.7 MeV) nuclei is valid. Under these conditions, the simulation of experimental data has been done with the help of RUMP [8] software package. The backscattering cross-sections of α particles on O and Si were taken from IBANDL library [9]. The results on the stoichiometry and thickness of sample PLD586

inferred from the simulated non-Rutherford α backscattering spectrum (**Figure 4**) are expressed by: hafnium 1.2% stabilized zirconia ($ZrO_2Hf_{0.012}$) and respectively $1{,}300\times10^{15}$ atoms/cm^2.

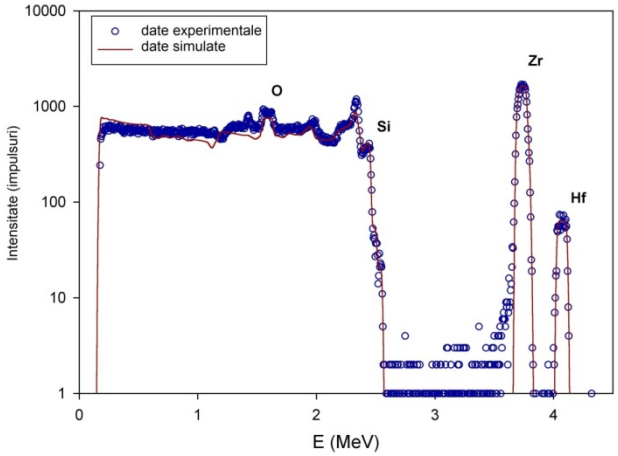

Figure 4. *NRBS spectrum of sample PLD586: blue (circle) – experimental data, red (continuous line) – simulated data.*

The ***optical investigation*** of synthesized ZrO_2 thin films relied on the following optical model: the Si(100) collector with a thickness of approximately 1 mm, a native SiO_2 layer 3- nm-thick, the ZrO_2 thin film, and the roughness layer taken as BEMA 50% ZrO_2 – 50% air. Since on the investigated spectral range 400 – 1700 nm zirconia is practically transparent [10], the computation of geometric and optical parameters was realized using a Cauchy fitting procedure where the refraction indices of Si(100) substrates and of native de SiO_2 layers were taken from literature [11]. The influence of substrate temperature on the dependence of the refraction index on wavelength was analyzed both in the absence of RF power (**Figure 5a**) and respectively in the presence of RF-assistance (**Figure 5b**). An increase of the substrate temperature produces an increase of the refraction index values for both PLD and RF-PLD techniques. Moreover, the comparison between the variation laws of the refraction index for two samples deposited under the same conditions excepting RF-assistance (**Figure 6**) proves superior optical properties in the presence of RF discharge.

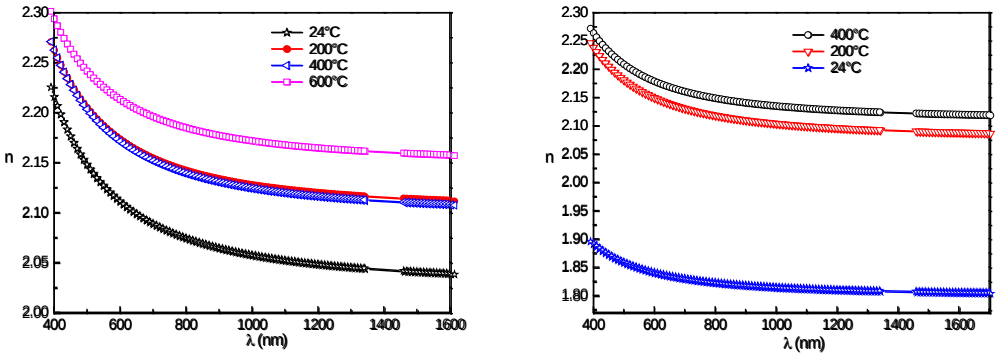

Figure 5. *Refractive indices in the case of: (a) (left) PLD technique – samples PLD575 (black), PLD569 (blue), PLD570 (red), and PLD573 (pink); (b) (right) RF-PLD technique – samples PLD576 (blue), PLD572 (red), and PLD571 (black).*

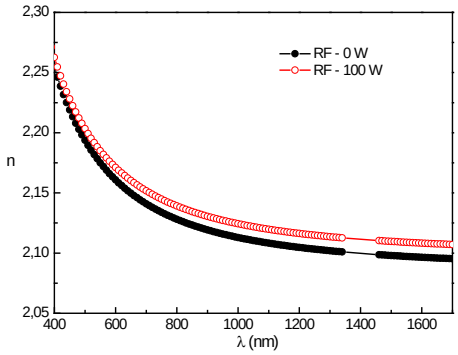

Figure 6. *Influence of RF-assistance on the refraction index: PLD570 (black) without RF and PLD571 (red) with RF.*

3.3. CONCLUSIONS

PLD and RF-PLD techniques allowed the formation of crystalline ZrO_2 thin films with applicative potential in nuclear waste management with the following properties: 1. Tetragonal zirconia crystalline phase is prevalently formed at a substrate temperature of at least 400 °C, in which context the peaks associated with the reflections t(101) and t(002) are the most visible; 2. Surface morphology modifies insignificantly under substrate temperature variations: spare droplets are observed and the RMS roughness values are stabilized to approximately 6 nm for all the films; 3. Average composition and thickness values of the zirconia layers following from alpha backscattering spectra are given by $ZrO_2Hf_{0.012}$ and respectively by 1300 x 10^{15} atoms/cm^2; 4. RF-assistance of the PLD process improves the surface quality by lowering the roughness values and droplet sizes simultaneously with a more pronounced film surface nanostructuring than in the case of conventional PLD; 5. Optimal optical properties are exhibited at 600 °C by RF-PLD (P_{RF}=100 W).

3.4. SELECTED BIBLIOGRAPHY

[1] W. L. GONG, W. LUTZE, R. C. EWING, *J. Nucl. Mater.* **277** (2000) 239–249.
[2] R. STEVENS, *Zirconia and zirconia ceramics*, Twickenham: Magnesium Elektron Ltd, 1986.
[3] L. THOMÉ, A. GENTILS, J. JAGIELSKI, F. GARRIDO, T. THOMÉ, *Nucl. Instr. Meth. B* **250** (2006) 106–113.
[4] L. THOMÉ, A. GENTILS, J. JAGIELSKI, F. GARRIDO, T. THOMÉ, *Vacuum* **81** (2007) 1264–1270.
[5] C. DEGUELDRE, *J. Alloys Compd.* **444-445** (2007) 36–41.
[6] P. SCHERRER, *Nachrichten von der Königlichten Gesellschaft der Wissenschaften zu Göttingen. Mathematisch-physikalische Klasse aus der Jahre 1918* (1918) 98–100.
[7] B. SCHMIDT, K. WETZIG, *Ion Beams in Materials Processing and Analysis*, Springer, 2013.
[8] L. R. DOOLITTLE, *Nucl. Instrum. Meth. B* **9** (1985) 344–351.
[9] http://www-nds.iaea.org/ibandl
[10] D. CIUPARU, A. ENSUQUE, G. SHAFEEV, F. BOZON-VERDURAZ, *J. Mater. Sci. Lett.* **19** (2000) 931–933.
[11] C. M. HERZINGER, B. JOHS, W. A. MCGAHAN, J. A. WOOLLAM, W. PAULSON, *J. Appl. Phys.* **83** (1998) 3323–3336.

4. FUNCTIONAL TITANIUM DIOXIDE THIN FILMS WITH APPLICATIONS TO BIONANOTECHNOLOGIES

TiO_2 nanostructures (inclusively in thin film form), due to the high values of their surface-to-volume ratios and of the observed hydrophilic or (photoinduced) super-hydrophilic behavior, raised an elevated interest within various new research topics from bionanotechnologies generated by microfluidic applications [1]: medical imaging, *in-vitro* diagnosis, nanotherapeutics, implantology, implementation of nanoagent biodistribution models in diagnosis and therapeutics [2,3,4]. In this context here we analyze the growth of functional TiO_2 thin films with applications to bionanotechnologies. The films have been synthesized by both PLD and MAPLE using Si(100) and respectively PPX-coated Si(100) substrates. PLD growths have been done with two laser systems: one ArF and the other Nd:YAG. In view of the MAPLE technique the targets were previously prepared by freezing some aqueous TiO_2 powder solutions of different weight concentrations. In this case a Nd:YAG laser system was employed. The deposited TiO_2 films have been investigated by XRD, AFM, SIMS, and SE. The effect of the substrate topography on the wettability properties of TiO_2 thin layers has been analyzed by contact angle measurements (CAM).

4.1. FILM SYNTHESIS

TiO_2 thin films have been synthesized by two methods – PLD and MAPLE, on two types of substrates: Si(100) and parylene-coated Si(100), the latter previously obtained by plasma polymerization. PLD growths were done with two laser systems: ArF (193 nm) and respectively Nd:YAG (1064 nm), the collectors being kept at room temperature. MAPLE depositions were implemented with a Nd:YAG (266 nm) laser system and required target preparation by freezing some aqueous TiO_2 solutions of 5 wt. % and respectively 10 wt. %. The experimental conditions of titania thin film preparation are synthesized in **Table 1**.

Table 1. *Experimental conditions used at the synthesis of TiO_2 thin films.*

Sample no.	Method	Target	Substrate	Oxygen pressure (mbar)	d_{t-s} (cm)	N_{pulses}	Φ (J/cm^2)	λ (nm)
1279a	PLD	TiO_2	Si(100)	0.01	4.0	80,000	3.0	193
1279b	PLD	TiO_2	PPX/Si(100)	0.01	4.0	80,000	3.0	193
1280a	PLD	TiO_2	Si(100)	0.01	4.0	40,000	3.0	1064
1280b	PLD	TiO_2	PPX/Si(100)	0.01	4.0	40,000	3.0	1064
164a	MAPLE	TiO_2 (10%)	Si(100)	vacuum	3.5	40,000	0.8	266
164b	MAPLE	TiO_2 (10%)	PPX/Si(100)	vacuum	3.5	40,000	0.8	266
165a	MAPLE	TiO_2 (5%)	Si(100)	vacuum	3.5	40,000	0.8	266
165b	MAPLE	TiO_2 (5%)	PPX/Si(100)	vacuum	3.5	40,000	0.8	266

4.2. RESULTS AND DISCUSSIONS

PLD-synthesized TiO_2 samples exhibit an amorphous behavior, most probably due to the low substrate temperatures during the growths (21 – 25 °C). The samples deposited by MAPLE, much thinner than those synthesized by PLD, required GI-XRD (grazing incidence XRD) technique for ***crystallographic determinations***. From Figures **1a** and **1b** (GI X-ray diffractograms of samples 164b and 165b deposited on PPX substrates by MAPLE correlated with those of the collectors) one observes a crystalline structuring only for films inferred from targets of higher titania concentrations (10 wt. % TiO_2, **Figure 1a**). The broad and not very accurate diffraction peak accredited to the anatase phase signalizes a low crystallinity degree along with a short-range crystallographic organization.

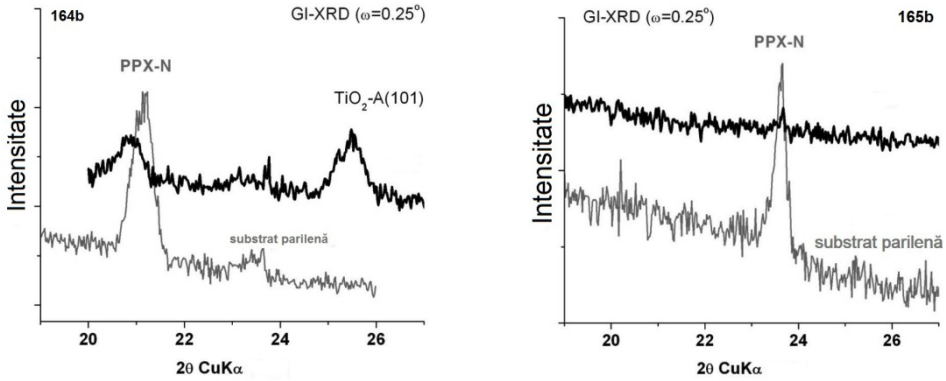

Figure 1. *Influence of target concentration on the crystallinity of TiO_2/PPX samples deposited by MAPLE: (a) (left) 10 wt. % TiO_2; (b) (right) 5 wt. % TiO_2.*

One of the essentials parameters of ***surface morphology*** properties of thin films is represented by the laser itself. Two samples deposited by PLD under the same conditions but the laser system are compared: 1279a (ArF, 193 nm, 40 Hz, 25 ns) and 1280a (Nd:YAG, 1064 nm, 10 Hz, 5 – 7 ns) – **Figure 2**. The ArF beam favors much smaller roughness values on all scanning areas (0.3 nm on 2x2 μm^2 and 1.5 nm on both 10x10 μm^2 and 20x20 μm^2) if compared with the Nd:YAG laser (3.1 nm on 2x2 μm^2, 7 nm on 10x10 μm^2, and 12 nm on 20x20 μm^2). From the images taken on a small scanning area (2x2 μm^2) it can be seen that the Nd:YAG beam provides the formation of droplets with micron magnitude order diameter and grains displaying characteristic diameters in the range 40 – 100 nm, while the ArF beam ensures a uniform, smooth nanostructure synthesis, also defect-free.

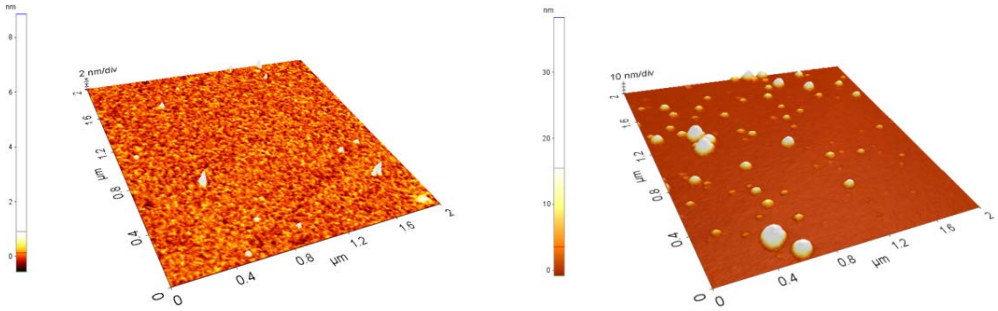

Figure 2. *Influence of laser system on the morphology of TiO_2/Si(100) thin films deposited by PLD: (a) (left) 1279a, ArF (193 nm) – RMS: 0.3 nm; (b) (right) 1280a, Nd:YAG (1064 nm) – RMS: 3.1 nm.*

For samples deposited by MAPLE on PPX substrates an increase of the TiO_2 target concentration from 5% to 10% is manifested through an increase of the roughness from 14 to 32 nm on 2x2 μm^2 (**Figure 3**), from 52 to 83 nm on 10x10 μm^2, and also from 56 to 123 nm on 20x20 μm^2, mainly due to the more pronounced titania grain accumulation from the target onto the substrate. The detailed AFM image (**Figure 3**) highlights that for a lower value of TiO_2 target concentration (5%) regular grains with dimensions of approximately 50 nm are present, while doubling the concentration yields a non-regular character of the observed nanostructures. The same type of behavior is noticed with respect to the influence of TiO_2 target concentration on the morphology of titania samples synthesized under the same conditions by MAPLE, but onto Si(100) collectors.

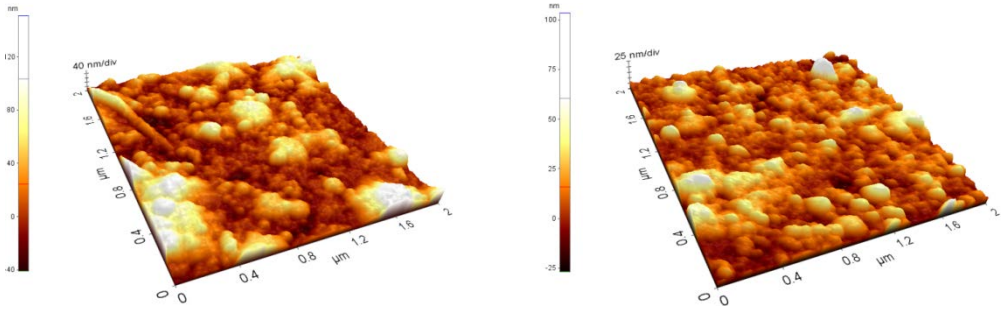

Figure 3. *Influence of target concentration on the morphology of TiO_2/PPX samples deposited by MAPLE: (a) (left) 164b (10 wt. % TiO_2, RMS: 32 nm); (b) (right) 165b (5 wt. % TiO_2, RMS: 14 nm).*

Micro-structural investigations of TiO_2 samples grown on Si(100) substrates were done by recording the intensities of ^{16}O, ^{28}Si, and ^{48}Ti signals. In **Figure 4** are included the depth profiles of two samples synthesized by PLD with different laser systems: ArF (193 nm) and respectively Nd:YAG (1064 nm) and in **Figure 5** for two films prepared by MAPLE (Nd:YAG, 266 nm) from targets of different TiO_2 concentrations.

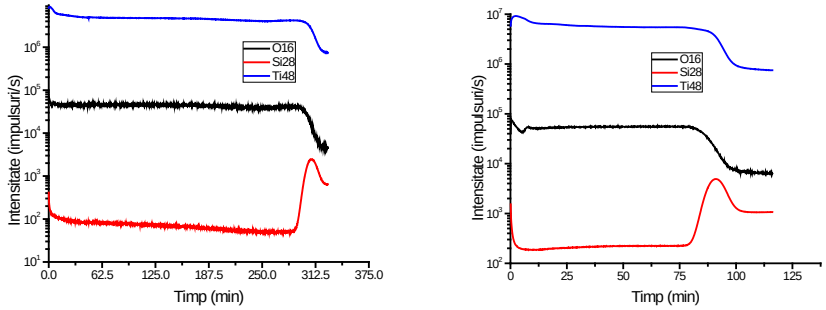

Figure 4. *Influence of laser system on the micro-structure of TiO_2/Si(100) thin films deposited by PLD. Depth profiles: (a) (left) sample 1279a, ArF (193 nm); (b) (right) sample 1280a, Nd:YAG (1064 nm).*

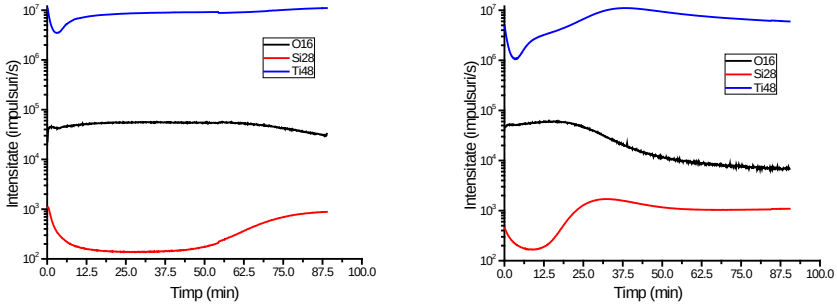

Figure 5. *Influence of target concentration on the micro-structure of TiO_2/Si(100) thin films deposited by MAPLE. Depth profiles: (a) (left) sample 164a (10 wt. % TiO_2); (b) (right) sample 165a (5 wt. % TiO_2).*

While PLD-grown samples show a relatively uniform distribution among their constituents irrespective of the laser system, those PLD-deposited emphasize a clear imbalance among their in-depth elements, irrespective of the target concentration. It seems that the samples synthesized by PLD allow relatively constant densities and insignificant roughness values compared to the film thicknesses, while the samples produced by MAPLE provide thinner TiO_2 films endowed with roughness layers of thickness comparable to the film thickness itself, but with lower densities and non-uniform titania distributions.

The ***optical investigations*** were carried out within the spectral range 400 – 1,000 nm with a step of 2 nm and at an incidence angle fixed at 70°. The optical model for sample 1280a synthesized by PLD is composed of: the silicon collector (1 mm), a native SiO_2 layer (3 nm), the TiO_2 thin film, and the roughness layer (BEMA 50% TiO_2 – 50% air) accompanied by a two-parameter Cauchy fitting. The optical properties of this film are given in **Figure 6a** (red), where a theoretical curve (black) from the literature [5] is included for comparison. It can be observed that the modeled values of the refraction index are comparable with those from the literature. Related to sample 165a synthesized by MAPLE the optical model is similar to the previous one: the silicon collector (1 mm), a native SiO_2 layer (3 nm), the TiO_2 thin film, and the roughness layer (BEMA 50% TiO_2 – 50% air). This film was assumed also with Cauchy dispersion, but with Urbach absorption. The optical properties (*n* and *k* variation laws) following from combined Cauchy-Urbach fitting are given in **Figure 6b**. The comparison with other results [5] proves higher values of *k* simultaneously with lower values of *n* than those specific to titania. The comparable values between the film thickness (40 nm) and that of the roughness layer (46 nm) are in complete agreement with AFM and SIMS analyses and confirm the porous aspect of this surface.

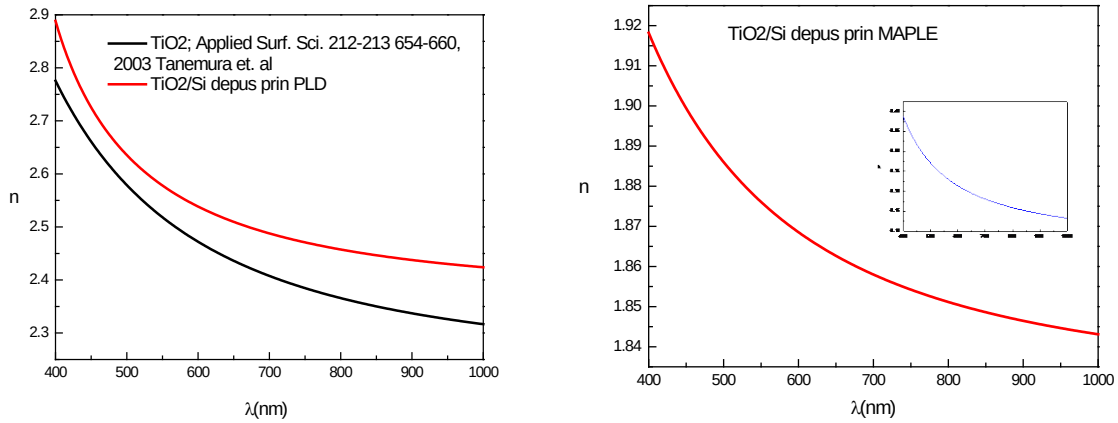

Figure 6. *(a) (left) Refractive indices in the case of: sample 1280a, Cauchy fitting (red); theoretical data (black). (b) (right) Graphical representations of n (red) and k (insertion, blue) for sample 165a, Cauchy-Urbach fitting.*

In conclusion, from the perspective of optical quality the PLD synthesis provides better results (lower roughness values, refraction indices in agreement with those known from the literature, small extinction coefficients on an large spectral domain), while MAPLE-based depositions produce rougher surfaces, with enhanced porosity and therefore with high values

of the specific surfaces, which recommend them to various applications in nanomedicine and bionanotechnologies.

TiO_2 thin films produced by laser techniques exhibit interesting properties from the perspective of their applications to bionanotechnologies and nanomedicine [6,7]. In this context the hydrophilic behavior [8,9,10] of their surfaces is essential since hydrophilic surfaces tend to attract the water molecules from the environment and therefore facilitate the development of biological systems onto themselves. In view of these considerations ***water contact angle measurements*** were done for all TiO_2 samples using Drop Profile Analysis Device CAM 200 from KSV Instruments Ltd. allowing for the detection of contact angles between 5º and 180º with an accuracy of 0.1º by means of the sessile drop static method. In this way the hydrophilic/hydrophobic character of each sample was established (**Table 2**). Seven out of the eight samples are hydrophilic, with values of the water mean contact angle between 43.13 ± 1.95º and 85.80 ± 1.20º, while one of the samples is weakly hydrophobic (94.15 ± 0.36º). For each pair of samples deposited under the same physical conditions the mean contact angle is systematically lower for PPX substrates than for Si(100) collectors.

Table 2*. Water mean contact angle measurements for TiO_2 thin films – sessile drop method.*

Sample	Mean contact angle (degrees)	Standard deviation (degrees)	Drop average volume (µL)	Volume standard deviation (µL)	Surface wettability
1279a	85.80	1.20	1.02	0.01	hydrophilic
1279b	82.70	1.39	1.16	0.01	hydrophilic
1280a	79.62	1.33	0.88	0.01	hydrophilic
1280b	77.09	3.20	1.32	0.01	hydrophilic
164a	**94.15**	**0.36**	**1.82**	**0.10**	**hydrophobic**
164b	**43.13**	**1.95**	**1.75**	**0.04**	**hydrophilic**
165a	80.18	0.92	1.47	0.02	hydrophilic
165b	73.04	3.71	1.71	0.19	hydrophilic

Figure 7 provides the graphical translation of the above table. It is worth noticing that we succeeded in synthesizing significantly hydrophilic TiO_2 thin films (under 45º) without additional UV treatments, simply by means of the MAPLE technique in the presence of a Nd:YAG system (266 nm) starting from a 10 wt. % TiO_2 target collected on PPX.

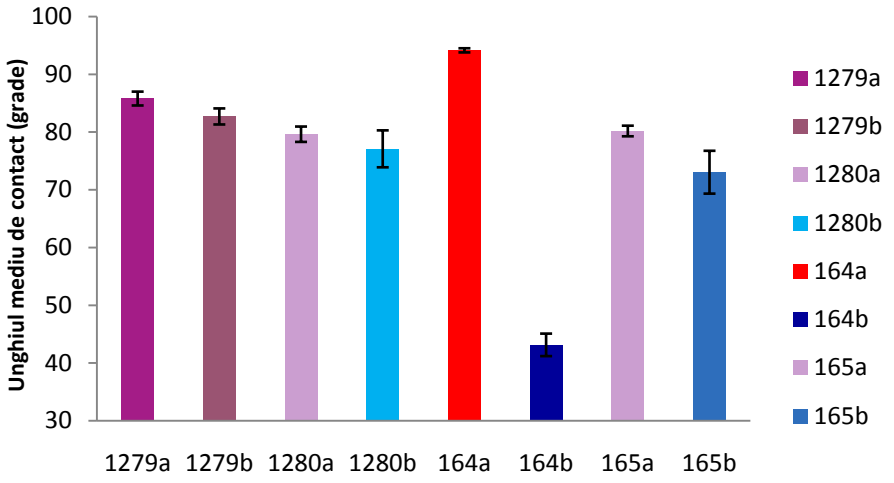

Figure 7. *Graphical translation of the water mean contact angle values of TiO_2 thin films inferred by sessile drop method.*

Thus, TiO_2 thin films adequate to further investigations by cell biocompatibility tests in view of their applications to bionanotechnologies and nanomedicine are those prepared by MAPLE on PPX collectors from targets with a relatively high TiO_2 weight concentration.

4.3. CONCLUSIONS

The main conclusions are as follows: 1. Morphology of titania films grown by PLD is characterized by smooth, uniform surfaces, whose roughness increases with an increase in the laser operating wavelength. On the other hand, MAPLE favors an increase of the film roughness with the TiO_2 target concentration irrespective of the substrate morphology; 2. PLD synthesis ensures a more balanced film composition by contrast to the inhomogeneous depositions produced by MAPLE; 3. Crystallinity lacks or is rather poor. Anatase phase is identified, but only for MAPLE growths from high concentration TiO_2 targets; 4. PLD-emerging samples exhibit very small values of their extinction coefficients together with values of the refraction index close to those reported in the literature, while MAPLE-grown films are less transparent and with lower values of the refraction index on a broad spectral range; 5. Substrate properties decisively influence the TiO_2 film wettability: parylene-coated Si(100) collectors lead to more hydrophilic surfaces than plain Si(100) supports.

4.4. SELECTED BIBLIOGRAPHY

[1] N. LIU, H. LI, H. WANG *el al.*, *Matt. Lett.* **89** (2012) 247–250.
[2] S. VENKATRAMAN, *Nanotechnology* **25** (2014) 372501.
[3] S. E. MCNEIL, *J. Leuk. Biol.* **78** (2005) 585–594.
[4] Z. AGUILAR, *Nanomaterials for medical applications*, Elsevier, 2013.
[5] S. TANEMURA, L. MIAO, P. JIN *el al.*, *Appl. Surf. Sci.* **212-213** (2003) 654–660.
[6] H.-J. OH, J.-H. LEE, Y.-J. KIM *el al.*, *Mater. Chem. Phys.* **109** (2008) 10–14.
[7] M. ZUBER, S. TABASUM, T. JAMIL *el al.*, *J. Appl. Polym. Sci.* **131** (2014) DOI:10.1002/app.39806.
[8] R. WANG, K. HASHIMOTO, A. FUJISHIMA *et al.*, *Nature* **388** (1997) 431–432.
[9] R. WANG, N. SAKAI, A. FUJISHIMA *el al.*, *Phys. Chem. B* **103** (1999) 2188–2194.
[10] D. H. SHIN, T. SHOKUHFAR, C. K. CHOI *el al.*, *Nanotechnol.* **22** (2011) 315704.

5. FUNCTIONAL TITANIUM DIOXIDE THIN FILMS WITH BIO-MEDICAL APPLICATIONS

Titania nanostructured coatings and thin films play a special role in biomedical applications focused on orthopedics and dentistry (bone tissue engineering) [1]. Some special titanium alloys exhibit physical and biocompatibility properties that induce their large scale usage in manufacturing orthopedic prostheses and dental implants [2]. Their TiO_2 passivation layer may undergo various treatments or may be replaced by coating or deposition of a titania thin layer in order to avoid the fibrous encapsulation of implants and meantime enhance the bone contact (osseointegration) [3].

The present chapter is focused on on the preparation of functional TiO_2 thin films with applications to implantology and prosthetics. Such thin layers have been synthesized by PLD with an ArF laser on three types of substrates: BK7 optical glass, Si(100), and quartz. Their physical characterization has been instrumented by XRD, AFM, SIMS, and SE. The accompanying bio-medical properties have been investigated via four *in-vitro* biocompatibility tests of a cell line L929 grown on the surfaces of the samples collected on optical glass: adherence, viability, and detection of the TiO_2 film genotoxic potential by means of alkaline comet and respectively cytokinesis-block micronucleus assays.

5.1. FILM SYNTHESIS

Titania thin films have been synthesized by PLD or RF-PLD with an argon fluoride laser (TiO_2 99.6% ceramic target) on three types of substrates: Si(100), optical glass (BK7), and quartz. The deposition experiments are schematically presented in **Table 1**.

Table 1. *Experimental conditions used at the synthesis of TiO_2 thin films.*

Sample no.	Target	Substrate	Oxygen pressure (mbar)	d_{t-s} (cm)	$T_{subst.}$ (°C)	E_{laser} (mJ)	N_{pulses}	Spot area (mm^2)	Φ (J/cm^2)	P_{RF} (W)	λ (nm)
1223a	TiO_2	glass	vacuum	4	RT	24	80,000	0.7	3.4	0	193
1223b	TiO_2	Si(100)/ photoresist	vacuum	4	RT	24	80,000	0.7	3.4	0	193
1224	TiO_2	glass	vacuum	4	300	24	80,000	0.7	3.4	0	193
1225	TiO_2	glass	vacuum	4	600	24	80,000	0.7	3.4	0	193
1226	TiO_2	glass	0.01	4	RT	24	80,000	0.7	3.4	0	193
1227a	TiO_2	quartz	0.01	4	RT	24	80,000	0.7	3.4	0	193
1227b	TiO_2	Si(100)	0.01	4	RT	24	80,000	0.7	3.4	0	193
1228	TiO_2	glass	0.01	4	300	24	80,000	0.7	3.4	0	193
1229	TiO_2	glass	0.01	4	600	24	80,000	0.7	3.4	0	193
1230a	TiO_2	glass	0.01	4	RT	24	80,000	0.7	3.4	100	193
1230b	TiO_2	Si(100)	0.01	4	RT	24	80,000	0.7	3.4	100	193
1231	TiO_2	glass	0.01	4	600	24	80,000	0.7	3.4	100	193
1232	TiO_2	glass	0.01	4	300	24	80,000	0.7	3.4	100	193

5.2. RESULTS AND DISCUSSIONS

Diffraction maxima have been identified with reference to the files PDF 00-044-1288 for cubic centered metallic Ti (β phase), 00-021-1272 for anatase TiO_2, and 00-021-1276 for rutile titania. The ***XRD analysis*** was done only for the samples synthesized on optical glass or quartz substrates and emphasized that the presence/accuracy of crystalline phases strongly depends on the collector temperature. Indeed, the lack of a crystallographic orientation on a large angular range indicates an amorphous behavior associated with low substrate temperatures (under 300 °C) for the films grown by PLD irrespective of other treatments. On the contrary, for sample 1225 (600 °C, vacuum) the β phase of metallic Ti is visible for the first time, even if not crystalline TiO_2. Maintaining the temperature at 600 °C and adding an O_2 background (**Figure 1a)** the presence of TiO_2 phases become visible (anatase and rutile), the best delimited maximum being attributed to the reflection A(004). Also at 600 °C and in O_2 background, but in the presence of RF assistance (**Figure 2a**), one notices the disappearance of the rutile phase simultaneously with an attenuation of metallic Ti phases, the best formed peak being accredited to the reflection A(101). Meanwhile, the crystallographic organization is improved with respect to the previous sample. Thus, it seems that the RF-PLD technique combined with high substrate values, of at least 600 °C, favors the formation of crystalline TiO_2 thin films, mainly anatase, with enhanced properties.

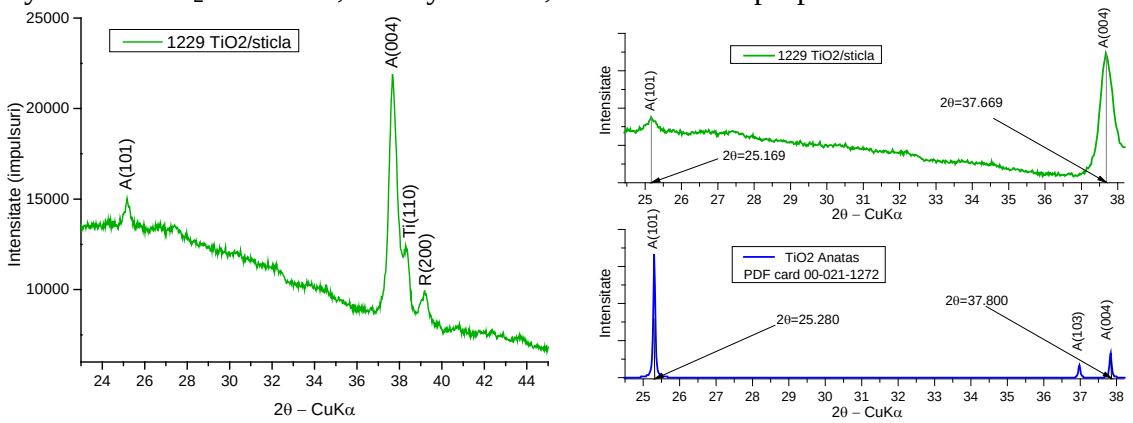

Figure 1. *X-ray diffractograms of sample 1229: (a) (left) crystalline phases; (b) (right) 2θ values for the peaks A(101) and A(004).*

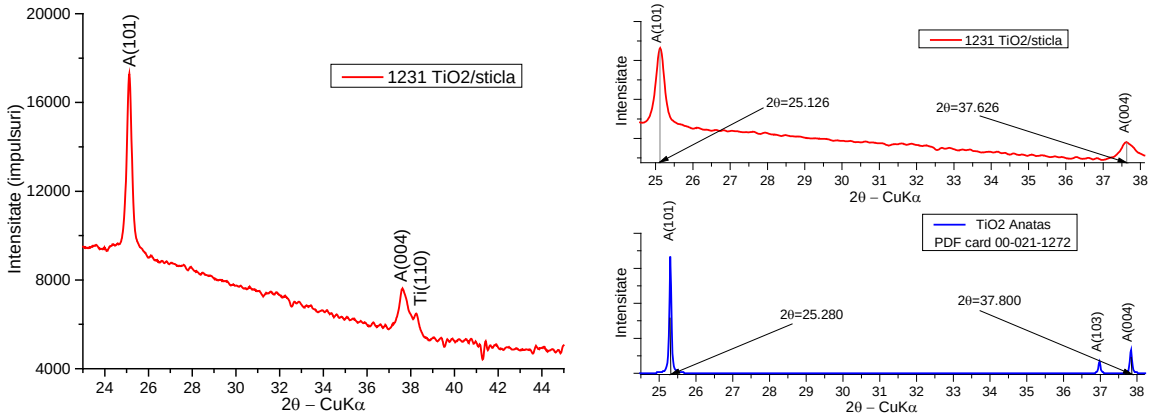

Figure 2. *X-ray diffractograms of sample 1231: (a) (left) crystalline phases; (b) (right) 2θ values for the peaks A(101) and A(004).*

The values of the 2θ angle corresponding to the diffraction maxima A(101) and A(004) for samples 1229 and 1231 are a little lower that the reference data (**Figure 1b** and **Figure 2b**), mainly due to the differences between the experimental conditions (temperature/pressure) under which the XRD measurements were carried out.

The AFM characterization of TiO_2 thin films proved that the deposition morphology is not affected by the substrate nature. In view of this, the influence of substrate temperature on the samples deposited in vacuum (**Figure 3** – 1223a, RT versus 1224, 300 °C) was initially investigated. On small scanning areas the nanostructuring tendency is manifest and also amplified with an increase in the collector temperature from RT to 300 °C; the RMS roughness varies from 0.58 nm to 0.2 nm. On higher areas the same samples exhibit a smooth aspect, with low grain densities, and without pores.

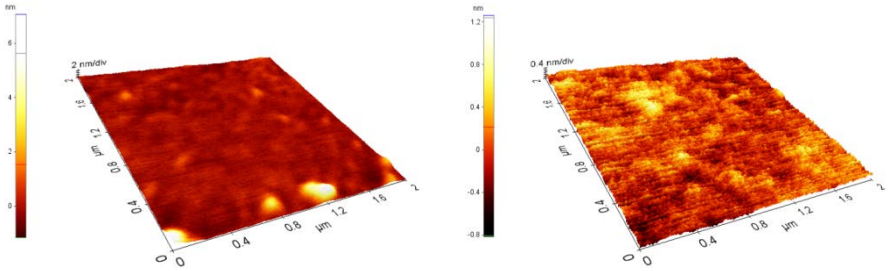

Figure 3. *Influence of substrate temperature on the morphology of titania thin films deposited in vacuum:(a) (left) 1223a – RMS: 0.58 nm; (b) (right) 1224 – RMS: 0.2 nm.*

For samples grown in O_2 background without RF, but at different temperatures – 1226 at RT and 1228 at 300 °C (**Figure 4**) – the nanostructuring tendency while increasing the temperature from RT to 300 °C is maintained. While at RT the surface displays sporadic grains, between 50 and 100 nm (**Figure 4a**) and a RMS roughness of 2.6 nm, at 300 °C there appear pore-like defects with a diameter of about 300 nm, so the RMS raises to 7.4 nm. Not only the temperature raise is responsible for pores, but also the presence of reactive gas under pressure, as follows from **Figure 3b** (sample 1224, also deposited at 300 °C, but in vacuum, exhibits no pores).

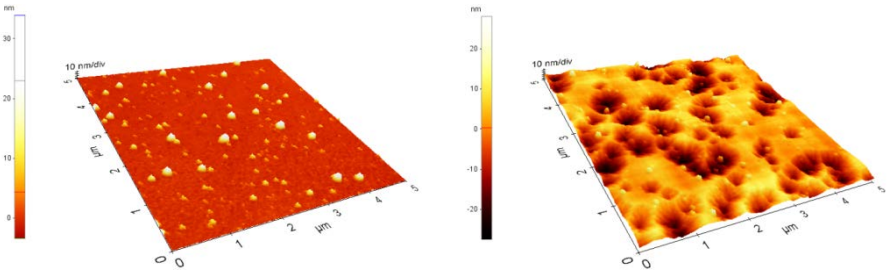

Figure 4. *Influence of substrate temperature on the morphology of titania thin films deposited in O_2 background:(a) (left) 1226 – RMS: 2.6 nm; (b) (right) 1228 – RMS: 7.4 nm.*

In the case of O_2 background preparation combined with RF assistance under different temperatures (**Figure 5** – 1231, 600 °C and 1232, 300 °C) the high substrate temperatures, of minimum 300 °C, corroborated with the presence of O_2 generates surface pores. Their diameter decreases with an increase of the temperature (from 400 nm – 300 °C at 200 nm – 600 °C). The amplification of surface nanostructuring with an increase of the temperature is also observable.

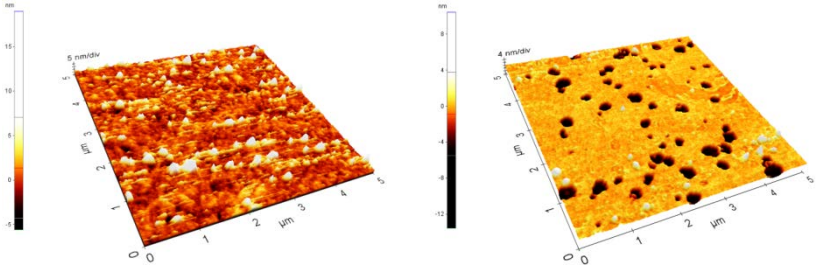

Figure 5. *Influence of substrate temperature on the morphology of titania thin films deposited by RF-PLD: (a) (left) 1231 – RMS: 2.1 nm; (b) (right) 1232 – RMS: 1.4 nm.*

Thus, the production of TiO_2 thin films with superior morphological properties necessitates a high substrate temperature, of at least 600 °C, in parallel with the admission of oxidant gas under pressure and RF assistance.

SIMS micro-structural characterization highlighted that neither the nature nor the temperature of the collector affects the in-depth composition of TiO_2 films. The essential parameter is given by the pressure of oxidant gas together with the enhancement of reactive species by RF plasma discharges. In this sense we compare the depth profiles of the ionic signals due to the isotopes ^{16}O (black), ^{28}Si (red), and ^{46}Ti (blue) for three samples deposited at 300 °C: 1224 in vacuum, 1228 in O_2 background, no RF and 1232 in O_2 background, with RF (**Figure 6**). In the absence of RF discharges (**Figure 6a** and **Figure 6b**) the films are homogeneous, the recorded ^{16}O and ^{46}Ti signals displaying an almost constant behavior on the investigated range. The RF assistance (**Figure 6c)** intensifies the substrate reactivity and therefore all signals vary strongly, proving thus an obvious imbalance among these in-depth components, which suggests the formation of an inhomogeneous film, with a multi-layer substructure. Films grown in O_2 background are thicker than those deposited in vacuum, so the oxidant atmosphere is responsible for a better growth stoichiometry.

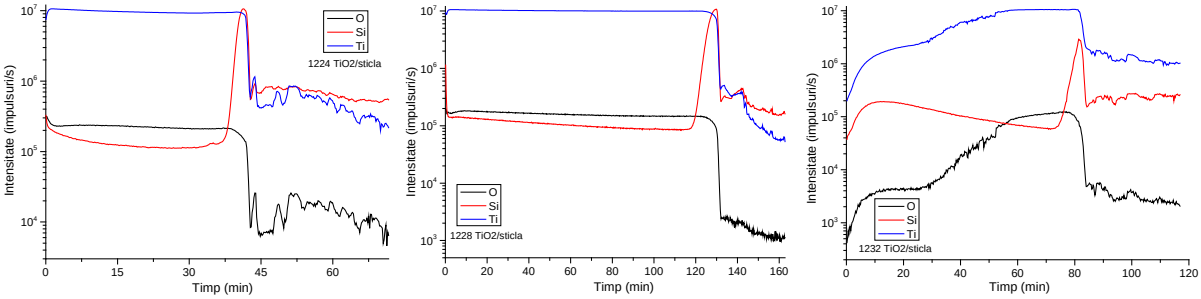

Figure 6. *Depth profiles of TiO_2/glass thin films at 300 °C, illustrating different homogeneity degrees: (a) (left) 1224 – vacuum; (b) (middle) 1228 – O_2 background, no RF; (c) (right) 1232 – O_2 background, with RF.*

The ***investigation of geometric/optical properties*** of TiO_2 thin films debuted by recording their spectral transmission curves. In this way we observed that the films prepared in oxygen background by RF-PLD are practically transparent within the range 400 – 1200 nm irrespective of substrate nature or temperature. The influence of the collector nature on the geometric and optical parameters has been studied with respect to two samples deposited by RF-PLD under the same conditions but the substrate: 1230a/optical glass and 1230b/Si(100). The experimental data were collected on a reduced spectral range, 400 – 1200 nm, with a step of 2 nm and at an incidence angle fixed at 70°. The transmittance measurements show that both samples can be taken to be transparent on the entire investigated spectral range and in view of this we assumed a normal, Cauchy dispersion law with respect to the refraction index. The Cauchy fitting of experimental data was done in conjunction with the following optical models: 1230a/glass – a 1-mm-thick glass substrate, the TiO_2 film, and a roughness layer (50% air – 50% TiO_2); 1230b/Si(100) – a 1-mm-thick Si(100) collector, a native SiO_2 layer of 3 nm, the TiO_2 film, and a roughness layer (50% air – 50% TiO_2). The reference values of the refraction indices for Si and SiO_2 were taken from the literature [4], whereas for BK7 optical glass from the Schott database [5]. The Cauchy modeling generates the graphic of *n* for both samples (**Figure 7**). It can be seen that the values of the refraction indices are

relatively close on the entire range and also comparable with those known from the literature [6]. Since in addition the film thickness and roughness have close values for both samples, it follows that the geometric/optical properties of TiO_2 thin films synthesized by RF-PLD are not influenced by the substrate nature.

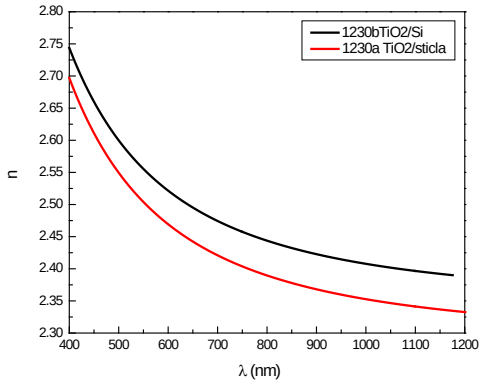

Figure 7. *Refractive indices in the case of two samples deposited on different substrates: 1230a on optical BK7 glass (red) and 1230b on Si(100) (black).*

In view of establishing the biomedical potential (implantology, prosthetics) of the prepared TiO_2 nanostructures ***four in-vitro biocompatibility tests*** were carried out: a morphological one dedicated to the evaluation of adherence of a certain cell line to the thin films, one designed for the determination of the metabolic cell activity (viability) in the presence of titania surfaces and two analyses specialized in the identification of the genotoxic potential of TiO_2 samples (alkaline comet assay and cytokinesis-block micronucleus assay). Seven samples deposited on optical glass substrates have been selected: 1223a (vacuum, RT), 1224 (vacuum, 300 °C), 1226 (O_2, RT), 1228 (O_2, 300 °C), 1229 (O_2, 600 °C), 1230a (O_2, RT, RF), and 1232 (O_2, 300 °C, RF). All tests have been implemented with cells pertaining to the L929 cell line (mouse fibroblasts, Sigma-Aldrich).

The ***in-vitro evaluation of cell adhesion*** has undergone according to the protocol described in chapter 2. After an incubation period of 20 hours on the sample surfaces and on the plastic control accompanied by Acridine Orange staining, the L929 cells were visualized with the aid of an optical fluorescence microscope Olympus BX51 equipped with an adequate filter. The adherence test was effectuated three times under the same conditions. A selection of the acquired images is included in the next figure.

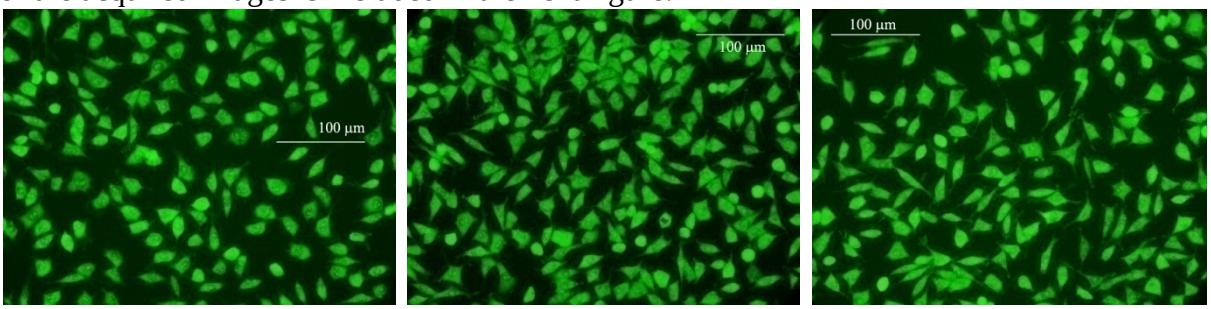

Figure 8. *In-vitro adherence of cells L929: (a) (left) on the plastic control; (b) (middle) on sample 1223a; (c) (right) on sample 1232.*

The cell-spread ratio, defined like in chapter 2, has been determined for each sample and for the control by means of the recorded images. The results have been processed statistically taken into account the number of experiments and the total number of minimum 300 cells per image and are presented in **Figure 9** as percentage averages and corresponding standard deviations. Excellent values of the cell-spread ratio have been obtained with respect to all

TiO_2 samples, within the range 79.31±4.35 – 90.44±4.46 %, compared with the control (92.86±1.76 %). The cell-spread ratio increases with an increase of the substrate temperature, the cell attachment being optimal in O_2 background and in the presence of an *in-situ* RF plasma discharge. The comparison with some results from the literature [7,8,9] indicates that the PLD technique allows the synthesis of TiO_2 thin films with superior cell attachment properties than other deposition methods.

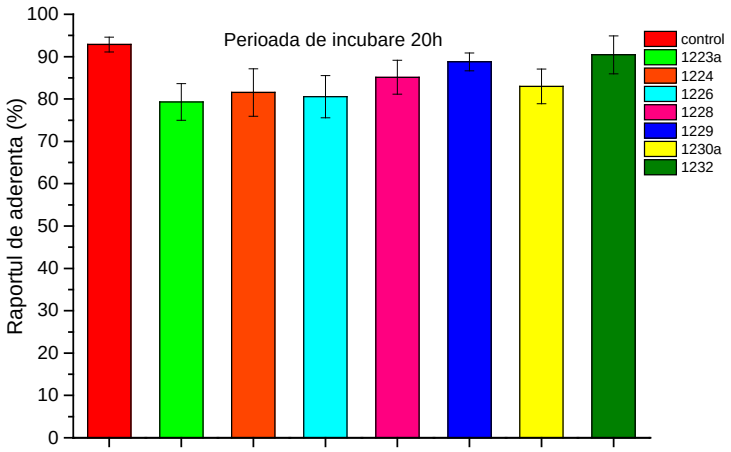

Figure 9. *Values of the cell-spread ratio of L929 cells.*

In-vitro evaluation of the viability of L929 cells in the presence of TiO_2 surfaces was implemented by Cell Titer 96® AQ_{ueous} Non-Radioactive Cell Proliferation Assay from Promega based on the dependence of the bio-reduction of MTS (a special class of tetrazolium inner salts) into a chemical product (cyan, soluble in growth media) known as formazan on the enzymatic (mitochondrial) metabolic cell activity [10,11]. Actually, there is assumed a linear relationship between the number of viable cells and the emerging quantity of formazan, where the latter is quantitatively identified by measuring the absorbance of the resulting formazan solutions at 490 nm (wavelength corresponding to the maximum of absorption spectra). After a 24-hour incubation period of a culture of 40,000 L929 cells onto the TiO_2 surfaces and onto the optical glass control and application of the standard bio-reduction protocol [12] for 4 hours, the absorbance of the aftermath formazan solutions at 490 nm was recorded with a plate reader Sunrise™ Basic Tecan and the data were processed with Magelan™ – Data Analysis Software taking into account the number of identical experiments performed (three) and are given in **Figure 10** via average absorbance values and corresponding standard deviations.

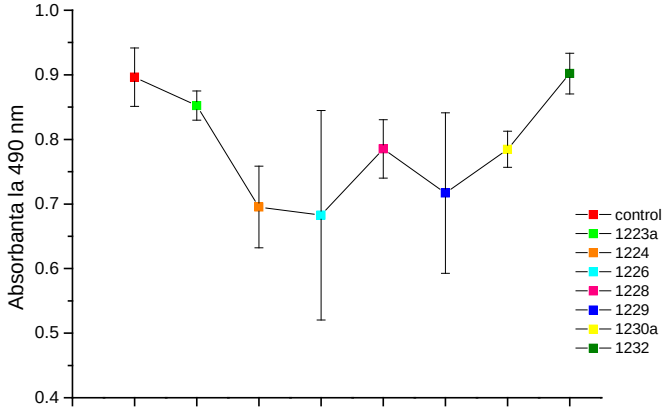

Figure 10. *Absorbance at 490 nm from the MTS assay.*

The highest two values of the number of viable cells (and also closest to control) follow from two different configurations: by RF-PLD, in O_2 background, at 300 °C and respectively by PLD, in vacuum, at RT. The analysis of the overall viability of TiO_2 samples with respect to the glass control results in a minimal percentage of 76% (by PLD, in O_2 background, at RT), meaning a very good result compared to those known from the literature [7,8,9].

In-vitro alkaline comet assay stands for a reliable test used here at the identification of the genotoxic potential of TiO_2 thin films with respect to the cell line L929, more precisely of single- and double-strand DNA breaks [13], based on single cell microgel electrophoresis. We applied the method developed by Singh [14] starting from a suspension of 20,000 L929 cells incubated for 48 hours on TiO_2 and glass control surfaces, followed by alkalinization (20 min.) and agarose gel electrophoresis (30 de min.) The cell slides have been stained with ethidium bromide and visualized with an Olympus BX51 microscope. As a result of this process the fragments of damaged DNA migrate to the anode and form characteristic comet images – **Figure 11**. The comet assay was done three times under identical conditions.

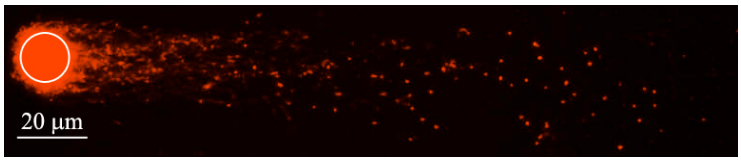

Figure 11. *Representative image of a L929 cell grown on sample 1224 (TiO_2/glass).*

The acquired comet images (minimum 100 per sample/control) have been processed with the software package Comet Assay IV and the relative intensity of the tail with respect to the head (proportional to the percentage of DNA damaged by single/double-strand DNA breaks) has been computed (**Figure 12**). The average values of tail intensity together with the standard deviations are included.

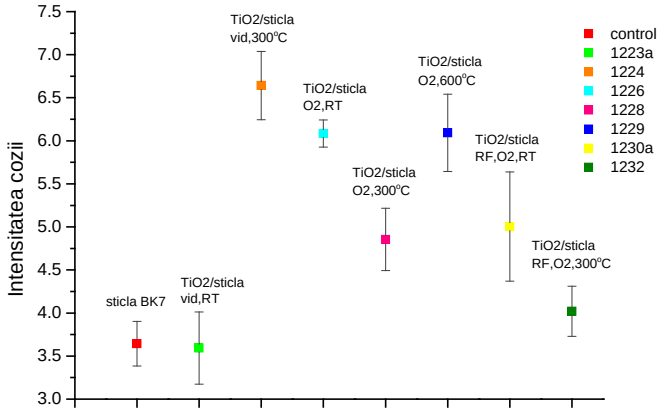

Figure 12. *Tail intensity for the comets originating in L929 cells grown on control and TiO_2/glass surfaces.*

The best values (with respect to the control) are inferred in the case of growths on TiO_2/glass thin films prepared under different conditions: by PLD, in vacuum, at RT and respectively by RF-PLD, in O_2 background, at 300 °C. The overall set of values proves that the TiO_2/glass samples obtained by pulsed laser ablation do not favor the damage of L929 cell DNA such as single/double-strand breaks. The results from the literature are strictly focused on TiO_2 nanoparticles and highlight their enhanced genotoxic potential, with few exceptions, like for instance in the context of a human lymphoblastoid TK6 cell population [15].

In-vitro cytokinesis-block micronucleus assay (CBMN) represents an innovative technique used here at the analysis of the genotoxic potential of TiO_2/glass films synthesized by PLD in the presence of L929 cells. Micronuclei – o class of nuclear cell anomalies [16] – are known as biological markers of genotoxic events and chromosomal instabilities and are detectable only during the anaphase stage of mitosis. The CBMN technique [17,18,19] requires the count of micronuclei at the level of binucleated cells at the end of a single cell division (cells grown in the presence of the substance whose genotoxic potential is investigated), obtained by cytokinesis-block in presence of Cytochalasin-B. Subcultures of 5,000 L929 cells have been grown for 24 hours on the surface of each TiO_2 sample and of the glass control. Then, a solution of Cytochalasin-B (3µg/mL) was added and the tissue culture test plate has been incubated for 17 hours (cell cycle doubling time). Subsequently, the cells were stained with Acridine Orange (0.03mg/mL) and visually counted with an optical microscope (Olympus BX51). A single experiment was carried out and the results, expressed as the number of micronuclei detected per 1,000 binucleated L929 cells, are collected in **Figure 13**.

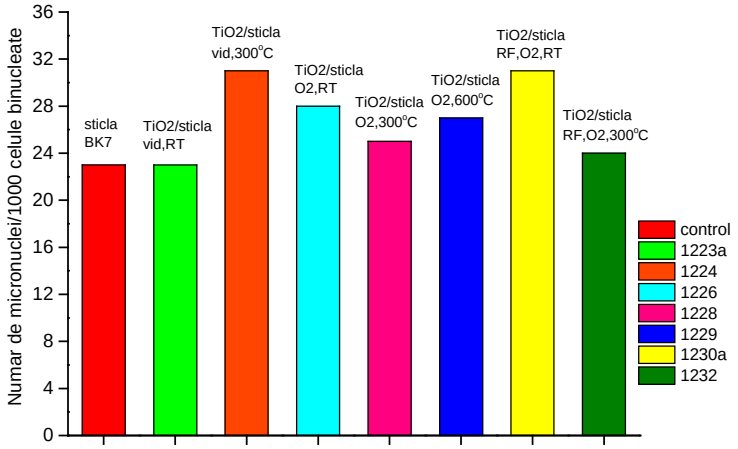

Figure 13. *Number of micronuclei per 1,000 binucleated L929 cells grown on control and TiO_2/glass surfaces.*

One notices excellent and very good results of the number of micronuclei per 1,000 binucleated L929 cells grown on TiO_2 sample surfaces (within the range 23 – 31) with respect to the control (23), which shows that the analyzed films are not genotoxic at the level of the L929 cell line from the point of view of DNA distribution during the cell cycles. The best two values (with respect to the control) have been recorded under the same conditions like before: by PLD, in vacuum, at RT and respectively by RF-PLD, in O_2 background, at 300 °C. A comparison with the results known from the literature [20–27] emphasizes that TiO_2/glass thin films synthesized by PLD or RF-PLD do not favor the *in-vitro* formation of micronuclei.

Putting together the results obtained so far at the level of the entire set of TiO_2/glass thin films prepared by pulsed laser ablation, we observe that the optimal *in-vitro* biocompatibility properties with respect to the L929 cells are manifested at a substrate temperature of 300 °C, in the presence of pressured oxidant gas (0.01 mbar), and under radio-frequency assistance (100 W).

5.3. CONCLUSIONS

The ablation configuration of the TiO_2/glass films that proved optimal with respect to the envisaged biomedical applications is characterized by: laser fluence – 3.4 J/cm^2, number of laser pulses applied on the target – 80,000, substrate temperature – 300 °C, in an O_2 background at 0.01 mbar, and with RF assistance (100 W). The main properties of the thin films prepared in this manner are synthesized by: 1. Formation of nanostructured surfaces with well-delimited pores presenting an average diameter of approximately 200 nm, a relatively high RMS roughness, of approximately 5 nm on a 20x20 μm^2 AFM scanning area, but without a noticeable crystalline organization; 2. Production of porous films with an inhomogeneous stratification, but with a better stoichiometry than in the case of samples deposited either in vacuum or without RF assistance; 3. Good optical properties, materialized in films transparent with respect to the visible and near IR radiation and possessing relatively high values of both the refraction index and transmittance; 4. Remarkable *in-vitro* biocompatibility features in the presence of L929 cell cultures, defined by A. an increased attachment level of these cell to the titania surfaces; B. an intense bioactivity (elevated viability); C. an inobservable genotoxic potential, as follows from the results of both alkaline comet and cytokinesis-block micronucleus assays.

5.4. SELECTED BIBLIOGRAPHY

[1] M. A. LOPEZ-HEREDIA, *Bioactivité d'implants en titan poreux produits par prototypage rapide*, Thèse de doctorat, Université de Nantes, 2008.

[2] M. A. LOPEZ-HEREDIA, E. GOYENVALLE, E. AGUADO *et al.*, *J. Biomed. Mater. Res. A* **85** (2008) 664–673.

[3] M. A. LOPEZ-HEREDIA, G. LEGEAY, C. GAILLARD, *et al.*, *Biomaterials* **29** (2008) 2608–2615.

[4] C. M. HERZINGER, B. JOHS, W. A. MCGAHAN *et al.*, *J. Appl. Phys.* **83** (1998) 3323–3336.

[5] Schott Optical Glass Data Sheets, December 2012, USA.

[6] S. TANEMURA, L. MIAO, P. JIN *et al.*, *Appl. Surf. Sci.* **212-213** (2003) 654–660.

[7] D. S. KOMMIREDDYA, S. M. SRIRAM, Y. M. LVOV, D. K. MILLS, *Biomaterials* **27** (2006) 4296–4303.

[8] X. XIANG, L. YAO, M. JIANG *et al.*, *Integr. Ferroelectr.* **136** (2012) 71–80.

[9] M. DHAYAL, R. KAPOOR, P. G. SISTLA *et al.*, *Mat. Sci. Eng. C* **37** (2014) 99–107.

[10] S. F. KHATTAK, M. SPATARA, L. ROBERTS, S. C. ROBERTS, *Biotechnol. Lett.* **28** (2006) 1361–1370.

[11] M. V. BERRIDGE, P. M. HERST, A. S. TAN, *Biotechnol. Annu. Rev.* **11** (2005) 127–152.

[12] PROMEGA CORPORATION, Cell Titer 96® AQ_{ueous} Non-Radioactive Cell Proliferation Assay – Instructions for use of products G5421, G5430, G5440, G1111 and G1112, Technical Bulletin **169** (2012) 1–15.

[13] W. N. CHOY (Editor), *Genetic toxicology and cancer risk assessment*, Marcel Dekker Inc., New York, 2001.

[14] N. P. SINGH, M. T. MCCOY, R. R. TICE, E. L. SCHNEIDER, *Exp. Cell Res.* **175** (1988) 184–191.

[15] R. S. WOODRUFF, Y. LI, J. YAN *et al.*, *J. Appl. Toxicol.* **32** (2012) 934–943.
[16] M. FENECH, M. KIRSCH-VOLDERS, A. T. NATARAJAN, *et al.*, *Mutagenesis* **26** (2011) 125–132.
[17] M. FENECH, A. A. MORLEY, *Cytobios* **43** (1985) 233–246.
[18] M. FENECH, A. A. MORLEY, *Mutat. Res.* **147** (1985) 29–36.
[19] M. FENECH, A. A. MORLEY, *Mutat. Res.* **161** (1986) 193–198.
[20] M. GHOSH, M. BANDYOPADHYAY, A. MUKHERJEE, *Chemosphere* **81** (2010) 1253–1262.
[21] Q. RAHMAN, M. LOHANI, E. DOPP *et al.*, *Environ. Health Persp.* **110** (2002) 797–800.
[22] T. CHEN, J. YAN, Y. LI, *J. Food Drug Anal.* **22** (2014) 95–104.
[23] Z. MAGDOLENOVA, A. COLLINS, A. KUMAR *et al.*, *Nanotox.* **8** (2014) 233–278.
[24] A. SARKAR, M. GHOSH, P. C. SIL, *J. Nanosci. Nanotechnol.* **14** (2014) 730–743.
[25] S. CHIBBER, S. A. ANSARI, R. SATAR, *J. Nanopart. Res.* **15** (2013), Article ID UNSP 1492, DOI: 10.1007/s11051-013-1492-x.
[26] I. IAVICOLI, V. LESO, A. BERGAMASCHI, *J. Nanomater.* **2012** (2012), Article ID 964381 (36 pag.), DOI: 10.1155/2012/964381.
[27] R. LANDSIEDEL, L. MA-HOCK, A. KROLL *et al.*, *Adv. Mater.* **22** (2010) 2601–2627.

6. CONCLUSIONS AND PERSPECTIVES

The general conclusion of this work is that *conventional techniques based on pulsed lasers (PLD, MAPLE) may be optimally controlled at the level of deposition parameters and treatments in view of zirconium and titanium oxide thin film synthesis with functional properties required at specific applications in cell and molecular biology, nuclear waste management, bionanotechnologies, and bio-medicine.* In what follows we systematize the results cumulated along the four chapters containing the author's original findings.

I. *Zirconia thin films with functional characteristics relevant to applications in cell and molecular biology* have been prepared by means of the PLD method. The optimal PLD synthesis of ZrO_2 thin films has been accomplished in the following configuration: at a laser fluence of 3.4 J/cm^2, by applying 80,000 laser pulses, at a substrate temperature of 600 °C, in O_2 background gas at 0.01 mbar, and in the presence of a RF plasma discharge power of 100 W. The main properties of the thin films prepared accordingly can be synthesized into:

1. Regular nanostructured surfaces, displaying a grain size distribution within the range 40 – 70 nm;
2. Polycrystalline monoclinic surfaces, thermodynamically stable;
3. Porous thin films with an inhomogeneous stratification;
4. Very good optical properties;
5. Chemical stability in the presence of typical antibiogram reactives;
6. Bacteriostatic effect in the presence of an Escherichia coli culture;
7. *In-vitro* biocompatibility properties manifested by a high adherence of L929 cells to the film surfaces.

II. It was emphasized that a relatively simple and low-cost technique such as PLD may be used at *the preparation of zirconia ceramics as crystalline thin films with applicative potential in the field of nuclear waste management*. The main characteristics of the resulting thin films may be briefly formulated into:

1. Tetragonal zirconia crystalline phase is prevalently formed at a substrate temperature of at least 400 °C, in which context the peaks associated with the reflections t(101) and t(002) are the most visible;
2. Surface morphology modifies insignificantly under substrate temperature variations: spare droplets are observed and the RMS roughness values are stabilized to approximately 6 nm for all the films;
3. Average composition and thickness values of the zirconia layers following from alpha backscattering spectra are given by $ZrO_2Hf_{0.012}$ and respectively by 1300 x 10^{15} atoms/cm^2;
4. RF-assistance of the PLD process improves the surface quality by lowering the roughness values and droplet sizes simultaneously with a more pronounced film surface nanostructuring than in the case of conventional PLD;
5. Optimal optical properties are exhibited at 600 °C by RF-PLD (P_{RF}=100 W).

III. PLD and MAPLE synthesis methods based on two laser systems (ArF/ Nd:YAG) allowed *the formation of titania thin films* on Si(100) and PPX collectors *providing*

functional properties recommending them to specific bionanotechnological applications, characterized by the following aspects:

1. Morphology of titania films grown by PLD is characterized by smooth, uniform surfaces, whose roughness increases with an increase in the laser operating wavelength. The MAPLE method favors an increase of the film roughness with the TiO_2 target concentration irrespective of the substrate morphology;
2. PLD synthesis ensures a more balanced film composition by contrast to the inhomogeneous depositions produced by MAPLE;
3. Crystallinity lacks or is rather poor. Anatase phase is identified, but only for MAPLE growths from high concentration TiO_2 targets;
4. PLD-emerging samples exhibit very small values of their extinction coefficients together with values of the refraction index close to those reported in the literature, while MAPLE-grown films are less transparent and with lower values of the refraction index on a broad spectral range;
5. Substrate properties decisively influence the TiO_2 film wettability: parylene-coated Si(100) collectors lead to more hydrophilic surfaces than plain Si(100) supports.

IV. Conventional PLD technique may be conveniently controlled at the level of deposition parameters and treatments in order to ensure *the synthesis of functional titanium dioxide thin films with bio-medical applications to implantology/prosthetics*. The optimal ablation configuration of the TiO_2/glass films is characterized by: laser fluence – 3.4 J/cm^2, number of laser pulses applied on the target – 80,000, substrate temperature – 300 °C, in an O_2 background at 0.01 mbar, and with RF assistance (100 W). The main properties of the thin films prepared in this manner are synthesized by:

1. Formation of nanostructured surfaces with well-delimited pores presenting an average diameter of approximately 200 nm, a relatively high RMS roughness, of approximately 5 nm on a 20x20 μm^2 AFM scanning area, but without a noticeable crystalline organization;
2. Production of porous films with an inhomogeneous stratification, but with a better stoichiometry than in the case of samples deposited either in vacuum or without RF assistance;
3. Good optical properties, materialized in films transparent with respect to the visible and near IR radiation and possessing relatively high values of both the refraction index and transmittance;
4. Remarkable *in-vitro* biocompatibility features in the presence of L929 cell cultures, defined by an increased attachment level of these cell to the titania surfaces, an intense bioactivity (elevated viability), and the absence of genotoxic potential, as follows from the results of both alkaline comet and cytokinesis-block micronucleus assays.

The results exposed so far allow for *interesting continuation perspectives at the level of synthesis, characterization, and properties of mixed TiO_2-ZrO_2 thin films in various proportions obtained by laser techniques.*

7. OVERALL PUBLICATIONS OF THE AUTHOR

I. PAPERS PUBLISHED IN ISI JOURNALS WITH IMPACT FACTORS AND ARTICLE INFLUENCE SCORE (AIS)

1. V. N. Cancea, V. Ion, M. Filipescu, F. Stokker-Cheregi, M. Dumitru, D. Colceag, M. D. Ionita, M. Dinescu, Effect of substrate composition and topography on the improvement of wettability of titanium dioxide thin films, *Journal of Optoelectronics and Advanced Materials* **16**(7-8) (2014) 804–811.
2. V. N. Cancea, M. Filipescu, G. Velisa, V. Ion, A. Andrei, D. Pantelica, R. Birjega, P. Ionescu, N. Scintee, M. Dinescu, Characterization of zirconia thin films grown by radio-frequency plasma assisted laser ablation, *Romanian Reports in Physics* **66**(4) (2014) 1137–1146.

II. PAPERS PUBLISHED IN ISI-INDEXED JOURNALS

1. V. N. Cancea, M. Filipescu, D. Colceag, C. Mustaciosu, M. Dinescu, Properties of zirconia thin films deposited by laser ablation, in *TIM 2012 Conference Proceedings*, 27-30 November 2012, Timişoara, Romania, *American Institute of Physics AIP Conference Proceedings* **1564** (2013) 138–146.

III. PAPERS PUBLISHED IN JOURNALS INDEXED IN OTHER DATABASES

1. V. N. Cancea, R. Birjega, V. Ion, M. Filipescu, M. Dinescu, Analysis of zirconia thin films grown by pulsed laser deposition, *Physics Annals of the University of Craiova PAUC* **22** (2012) 50–62, SCOPUS-indexed.
2. V. N. Cancea, V. Ion, M. Filipescu, M. Dinescu, Optical Properties of TiO_2 Thin Films Grown by PLD, *Physics Annals of the University of Craiova PAUC* **23** (2013) 18–27, SCOPUS- indexed.

IV. COMMUNICATIONS TO INTERNATIONAL CONFERENCES

1. V. N. Cancea, M. Filipescu, D. Colceag, C. Mustaciosu, M. Dinescu, Properties of zirconia thin films deposited by laser ablation, *TIM 2012 International Physics Conference*, 27–30 November 2012, Timişoara, Romania.
2. M. Filipescu, G. Velisa, V. Ion, A. Andrei, D. Pantelica, R. Birjega, P. Ionescu, N. Scintee, V. N. Cancea, M. Dinescu, Characterization of zirconia thin films grown by radio-frequency plasma assisted laser ablation, *CPPA 2013, 16th International Conference on Plasma Physics and Applications*, June 20–25 2013, Măgurele, Bucharest, Romania.
3. V. N. Cancea, M. Filipescu, F. Stokker-Cheregi, M. Dumitru, B. Mitu, M. D. Ionita, M. Dinescu, Effect of the composition and topography of substrates on

TiO_2 thin films deposited via laser techniques, COLA 2013, 12th International Conference on Laser Ablation, October 6–11 2013, Ischia, Italy.

4. V. N. Cancea, V. Ion, M. Filipescu, F. Stokker-Cheregi, M. Dumitru, D. Colceag, M. D.Ionita, M. Dinescu, Effect of substrate composition and topography on the improvement of wettability of titanium dioxide thin films deposited by multiple methods, *TIM 2013 International Physics Conference*, 21–24 November 2013, Timișoara, Romania.
5. V. N. Cancea, V. Ion, N. L. Dumitrescu, M. Dinescu, Optical properties of titanium dioxide thin films deposited by laser methods, *INDLAS 2014, 4th International Conference on Modern Laser Applications*, 19–23 May 2014, Bran, Romania.
6. V. N. Cancea, Properties of titanium dioxide thin films deposited by laser ablation, *TIM-14 Physics Conference – Physics without Frontiers*, 20–22 November 2014, Timișoara, Romania.